Biogeosciences, 23, 3467–3498, 2026
https://doi.org/10.5194/bg-23-3467-2026

Biogeosciences Open Access EGU

Chiral volatile organic compound fluxes from soil in the Amazon Rainforest across seasons

Johanna Margaretha Schüttler[1], Giovanni Pugliese[1], Joseph Byron[1], Cléo Quaresma Dias-Júnior[2], Carolina de A. Monteiro[1], Hartwig Harder[1], Jos Lelieveld[1,3], and Jonathan Williams[1,3]

[1]Max-Planck Institute for Chemistry, Mainz, Germany
[2]Climate and Environment Department, National Institute of Amazonian Research (CIAMB-INPA), Manaus, Brazil
[3]Climate and Atmosphere Research Center (CARE-C), The Cyprus Institute, Nicosia, Cyprus

Correspondence: Johanna Margaretha Schüttler (j.schuettler@mpic.de) and Jonathan Williams (jonathan.williams@mpic.de)

Received: 7 November 2025 – Discussion started: 21 November 2025
Revised: 18 February 2026 – Accepted: 19 April 2026 – Published: 21 May 2026

Abstract. The rainforest floor is an underexplored source and sink of biogenic volatile organic compounds (BVOC), and its contribution to the ecosystem BVOC budget remains poorly understood. We performed multi-seasonal measurements in the Amazon rainforest on the soil-atmosphere exchange of enantiomer-resolved monoterpenes ($C_{10}H_{16}$) and sesquiterpenes ($C_{15}H_{24}$), isoprene, and two isoprene oxidation products: methacrolein and methyl vinyl ketone. Soil uptake of isoprene and isoprene oxidation products was stronger during dry seasons than wet seasons and peaked in the afternoon hours. Sesquiterpene emission was highest during the El Niño-influenced dry season. Monoterpene fluxes showed changes in speciation across seasons. The presence or removal of the litter layer strongly altered the speciation of the monoterpene and sesquiterpene fluxes, partly shifting from emission with the litter layer to uptake without it. At the same time, the litter had no significant effect on isoprene. Enantiomeric ratios of α-pinene, limonene, β-pinene, and camphene differed between soil emissions and ambient air and shifted seasonally, suggesting distinct soil sources and processes. For each sesquiterpene only one enantiomer was detected. Although soil BVOC fluxes contribute little to the overall atmospheric budget in rainforests dominated by the plant canopy, they may affect near-surface chemistry and play important roles in (soil) ecology.

1 Introduction

The Amazon rainforest, Earth's largest tropical forest, releases a significant portion of carbon as biogenic volatile organic compounds (BVOC) to the atmosphere ($\sim 300\,\mathrm{Tg\,C\,yr^{-1}}$; Guenther et al., 2012). These BVOCs serve crucial ecological functions in vegetation response to abiotic (e.g., heat, drought, and oxidation) and biotic stress (e.g., pathogens and herbivores) as well as in the interactions between plants, animals, and microbes for communication (Kesselmeier and Staudt, 1999; Guenther et al., 2006; Gill and Tuteja, 2010; Ueda et al., 2012; Peñuelas et al., 2014; Staudt et al., 2017; Huang et al., 2019; Yáñez-Serrano et al., 2019, 2020; Honeker et al., 2023). Once emitted into the atmosphere, BVOCs rapidly react with oxidants such as ozone and hydroxyl radicals, thereby modulating oxidant levels and contributing to secondary organic aerosols (SOA) formation (Tripathi et al., 2025). SOA can grow to become cloud condensation nuclei (CCN) and, in turn, affect the Earth's radiative balance and climate (Andreae and Crutzen, 1997; Atkinson, 2000; Lelieveld et al., 2008; Williams, 2004). Among BVOCs, isoprene ($150\,\mathrm{Tg\,yr^{-1}}$) and monoterpenes (MTs $60\,\mathrm{Tg\,yr^{-1}}$) dominate emissions, while sesquiterpenes (SQTs), although less abundant, are highly reactive with ozone making them important for atmospheric chemistry processes (Bonn and Moortgat, 2003; Bourtsoukidis et al., 2012; Horváth et al., 2012; Yee et al., 2018; Barreira et al., 2021; Dada et al., 2023; Isaacman-VanWertz et al., 2024; Bourtsoukidis et al., 2025). Moreover, most MTs and SQTs are chiral, existing in two mirror-image forms known as enantiomers. Plants and other organ-

isms, like insects, often emit one enantiomer in excess, reflecting the dominant biosynthetic pathway in a species, a given tissue or a chemotype by using a stereoselective terpene synthase enzyme (Yassaa and Williams, 2007; Song et al., 2014; Staudt et al., 2019; Zannoni et al., 2020). The atmospheric reactivity of enantiomers towards ozone and OH radicals is identical. However, the further reaction and dimer formation might have stereochemical preferences for α-pinene and limonene enantiomers (Bellcross et al., 2021; Gao et al., 2025). Although chirality does not play a role in total atmospheric reactivity, organisms use specific enantiomers in order to communicate via the atmosphere to predators or conspecifics. The (−)-α-pinene enantiomer was found to play a role in plant-insect interactions, attracting beetles to already weaker trees (Norin, 1996). The (+)-α-pinene/(−)-α-pinene ratio can be elevated in response to mechanical stress (Eerdekens et al., 2009), and in spruce plants, a response to drought stress was found to result in higher emission rates of the (−)-enantiomers of limonene, β-phellandrene, α- and β-pinene (Daber et al., 2025). In a rainforest biome de novo synthesized (−)-α-pinene responded differently to increasing drought than (+)-α-pinene which is derived mainly from storage pools (Byron et al., 2022). Recently, it was shown that the enantiomeric ratio can be used to determine how the ecosystem responds to drought (Byron et al., 2025). Although an influence from the soil was not yet investigated. Yet enantiomer-resolved soil BVOC fluxes have not been reported.

While soils are increasingly recognized as sources and sinks of BVOCs, compared to canopy BVOC they remain poorly constrained. Understanding seasonal and diurnal patterns, as well as their enantiomeric resolution and environmental thresholds that control those fluxes is important for better assessing the impact of soil on ecology and atmospheric chemistry. Flux magnitudes and speciation are difficult to assess as they are the result of biotic, soil microbiome emissions and uptake as well as root exudates, and abiotic processes, like evaporation, diffusion, and sorption processes (Cleveland and Yavitt, 1997; Horváth et al., 2012; Rinnan and Albers, 2020). These processes in turn are sensitive to temperature, soil moisture, and soil porosity and interconnected with available ambient BVOCs and litter material, and therefore organic matter and nutrients, which can boost the microbial communities (Peñuelas et al., 2014; Weikl et al., 2016; Mäki et al., 2017; Kivimäenpää et al., 2018). Across ecosystems, soil BVOC fluxes are typically one to two orders of magnitude lower than canopy emissions, partly due to concurrent microbial uptake (Cleveland and Yavitt, 1997; Owen et al., 2007; Peñuelas et al., 2014; Drewer et al., 2021). Microbes can consume isoprene using it as an energy source, and may emit it at low rates (Cleveland and Yavitt, 1997; Gray et al., 2015; El Khawand et al., 2016; McGenity et al., 2018; Murrell et al., 2020). MTs can also be metabolized by soil microbes as a carbon source and can have an effect on pathways such as methanotrophy, nitrification, and denitrification in soil microbes (White, 1991, 1995). The isoprene oxidation product methyl vinyl ketone (MVK) was found as volatile metabolite from a bacteria and active against fungal spore germination (Herrington et al., 1987). Methacrolein (MACR) and MVK can both be directly emitted or uptaken by plants (Tani et al., 2010; Jardine et al., 2012; Fares et al., 2015). MT and SQT emissions in contrast were associated with plant roots (Mäki et al., 2017; Tsuruta et al., 2018), SQT especially also with soil fungi (Horváth et al., 2012), as well as with microbes (Asensio et al., 2008b; Weikl et al., 2016). In tropical forests, terpenoids are uptaken or emitted depending on the environmental conditions such as the soil water content, nutrient composition in soil, temperature, season, and vegetation (Bourtsoukidis et al., 2018; Llusià et al., 2022). Amazonian soils are reported to act as a strong source of SQTs under certain conditions (Bourtsoukidis et al., 2018). Soil BVOC fluxes in an artificial tropical forest have been reported to alter strongly under drought conditions (Pugliese et al., 2023).

El Niño climate events which occur semi-periodically (every 2–7 years) impact the Amazon rainforest by decreasing rainfall and elevating temperatures. It was shown in a modeling study that the isoprene emission flux increases as a response of the vegetation to a strong El Niño event (Vella et al., 2023). MT have also been shown to generally increase with temperature and due to drought stressed vegetation in tropical forest ecosystems (Byron et al., 2022; Gomes Alves et al., 2022; Werner et al., 2022). The 2023–2024 El Niño event caused a record drought in the Amazon rainforest (Espinoza et al., 2024). Climate projections indicate that the frequency and intensity of El Niño events are likely to increase under continued greenhouse gas emissions, with potentially profound effects on the Amazon and its BVOC dynamics (Geng et al., 2024).

In this study we investigated chirally resolved soil BVOC fluxes in the Amazon rainforest to assess the relevance of the soils to the total terpenoid BVOC budget in this ecosystem and see if soils have an influence on enantiomeric ratios. In particular, we are interested in the soil effect on the enantiomers of α-pinene, as these have been shown to be indicators of ecosystem drought stress (Byron et al., 2022, 2025), and a height gradient was observed at the ATTO tower site (Zannoni et al., 2020). We measured across four seasons, including the El Niño drought period in the dry season 2023 to account for and look into seasonal differences. Soil fluxes of isoprene, two of isoprene's oxidation products methyl vinyl ketone (MVK) and methacrolein (MACR), and enantiomer-resolved MTs and SQTs were quantified using thermal desorption-chiral gas chromatography-time of flight mass spectrometry (TD-GC-ToF-MS). The measurements were conducted at the Amazon Tall Tower Observatory (ATTO) research station (Andreae et al., 2015) located 150 km north east of Manaus (Brazil). The effect of temperature, soil moisture, soil properties, litter content and terpenoid ambient concentrations on soil terpenoid fluxes in

terms of local time of day, magnitude, flux direction (emission and/or uptake), and chemical composition, including chiral speciation was investigated.

2 Methods

2.1 Study site and sampling set-up

The experiments were conducted at the ATTO research facility in 2023 and 2024 across four seasons: from 22–26 January 2023 during the dry-to-wet transition season (dry-to-wet 2023), from 1–14 October 2023 during the dry season (dry 2023), from 24 April to 2 May 2024 during the wet season (Wet 2024), and from 11–20 October 2024 during the dry season (dry 2024). The ATTO site is a long-term measuring station in the Amazon Basin implemented to better the understanding of biosphere – atmosphere interactions (Andreae et al., 2015). The predominant wind direction from the northwest brings air masses from pristine rainforest with minimal human perturbation (Pöhlker et al., 2019). In the Amazon Basin the dry season with the lowest rainfall usually lasts from June to September and the wet season from January to April (Biscaro et al., 2021). The data presented here was taken at the end of each wet and dry season. The dry season in 2023 was influenced by an El Niño event with the result of a prolonged drought and higher than usual temperatures (Espinoza et al., 2024).

Soil VOC fluxes were measured from three manually operated soil chambers at six different times of the day: 05:00 am, 08:00 am, 11:00 am, 02:00 pm, 05:00 pm, and 08:00 pm local time. The three manual chambers were made from polyvinyl chloride (PVC), had a volume of 3.5 L, and consisted of a collar (ID: 19.4 cm, Area: 0.0295 m^2) and a lid equipped with a Teflon inlet and outlet (Fig. 1). The three PVC collars were installed at three different locations within a radius of 15 m to each other near the 325 m tall tower and at least 24 h prior to measurements. To avoid cutting roots, the collars were gently placed on the soil and sealed from the outside with soil taken from the area surrounding the collars. In January 2023 (dry-to-wet season 2023), the three chambers were installed on spot 1, spot 2, and spot 3 (Table 1). To investigate the effect of litter content on soil fluxes, the litter layer was removed from spot 3. Spot 1 was located near a termite nest. In October 2023 (dry season 2023), the chambers in spot 2 and 3 were moved to spot 4 and 5, where their litter layers were kept intact. Additional soil flux measurements without litter were performed from spot 5 in October 2024 (Table 1). Spot 4 and 5 were located within 15 m of spot 2 and 3. For soil flux measurements, the chamber lids were kept closed for 15 min before collecting samples, following a method used for cartridge measurements from a steady-state chamber within a study by Pugliese et al. (2023). Air was sampled on two sorbent cartridges in parallel: one connected at the outlet of the chamber; and one sampling the incoming ambient air near the chamber's inlet. The air volume was taken using a handheld pump (GilAir plus, Gilian) for 30 min at a flow rate of 200 mL min^{-1}, resulting in a total of 6 L of air collected. To prevent ozone from affecting the sampled VOCs, an ozone scrubber, consisting of a dried quartz filter soaked with a 10 % sodium thiosulfate solution, was placed in front of each cartridge during sampling. The ozone scrubbers were replaced after a maximum time of two weeks, as this time interval has been tested to be their minimum durability (Ernle et al., 2023).

To assess the effect of the chamber material on artifacts of the investigated soil BVOC fluxes, measurements were taken from a clean blank chamber. It was placed close to the other chambers on a soil spot where the bottom was covered in Teflon foil. A total of 23 replicates were measured from the blank chamber distributed across all seasons, and the mean blank fluxes and the standard deviation median are reported in Table A2 in Appendix A.

2.2 BVOC analysis – Thermal Desorption – Gas Chromatography – Time of Flight Mass Spectrometer (TD-GC-TOF)

The sorbent cartridges were made of silica-coated stainless-steel tubes (89 mm × 5.33 mm I.D., SilcoNert 2000, SilcoTek) containing 150 mg of Tenax® TA mesh range 80/100 (Supelco) and Carbograph® 5 TD mesh range 40/60 (Lara srl.). The sorbents were sealed with quartz wool and stainless-steel tension springs (Sigma Aldrich).

Prior to use, the cartridges were conditioned at 300 °C for 1 h while being flushed with pure nitrogen at 2 bar pressures (TC-20, Markes International). After sampling, the cartridges were stored in a freezer at −20 °C and analyzed within 60 d at the Max Planck Institute for Chemistry in Mainz, Germany. In each campaign a minimum of two cartridges were not sampled with a volume of air, but opened and closed at the site and transported along the sampled cartridges. These transport blank cartridges did not contain any of the target compounds (below LOD).

Sampled cartridges were desorbed using a thermal desorption unit (TD100-xr and UNITY xr, Markes International). The thermal desorption process consisted of two stages. In the first stage, the cartridges were dry-purged for 5 min and then desorbed for 10 min at 250 °C. The desorbed sample was pre-concentrated onto a cold trap (Material Emissions, Markes International). In the second stage, the cold trap was first purged for 1 min at 30 °C and then injected at 250 °C for 5 min into the gas chromatograph (GC, Agilent Technologies 7890B) equipped with a 60 m long chiral β-DEX™ 120 capillary column (Sigma Aldrich) with an inner diameter of 250 µm and a film thickness of 0.25 µm. Helium 5.0 was used as a carrier gas at 1.2 mL min^{-1} flow rate. The GC oven temperature was initially held at 50 °C for 5 min, then ramped at 1.5 °C min^{-1} to 110 °C, followed by a ramp at 10 °C min^{-1} to 220 °C, where it was held for 10 min.

Table 1. Overview of measurement campaigns with attributed season, Oceanic Niño Index representing 3-month average temperature anomaly in the oceanic surface waters around the respective measurement period (NOAA's Climate Prediction Center, 2026), start date, end date, measured chambers and the number of flux data points.

Name in plots	Season	Oceanic Niño Index	Start Date (yyyy-mm-dd)	End Date (yyyy-mm-dd)	Number of flux data points	Chambers Measured
Jan 2023	Dry-to-wet	−0.5 (La Niña/Neutral)	2023-01-22	2023-01-26	20	Spot 1, Spot 2, Spot 3 without litter
Oct 2023	Dry	1.8 (around El Niño peak)	2023-10-01	2023-10-14	39	Spot 1, Spot 4, Spot 5
Apr–May 2024	Wet	0.8 (El Niño influenced)	2024-04-24	2024-05-02	35	Spot 1, Spot 4, Spot 5
Oct 2024	Dry	−0.2 (Neutral)	2024-10-11 2024-10-18	2024-10-20 2024-10-20	37 6	Spot 1, Spot 4, Spot 5 Spot 5 without litter

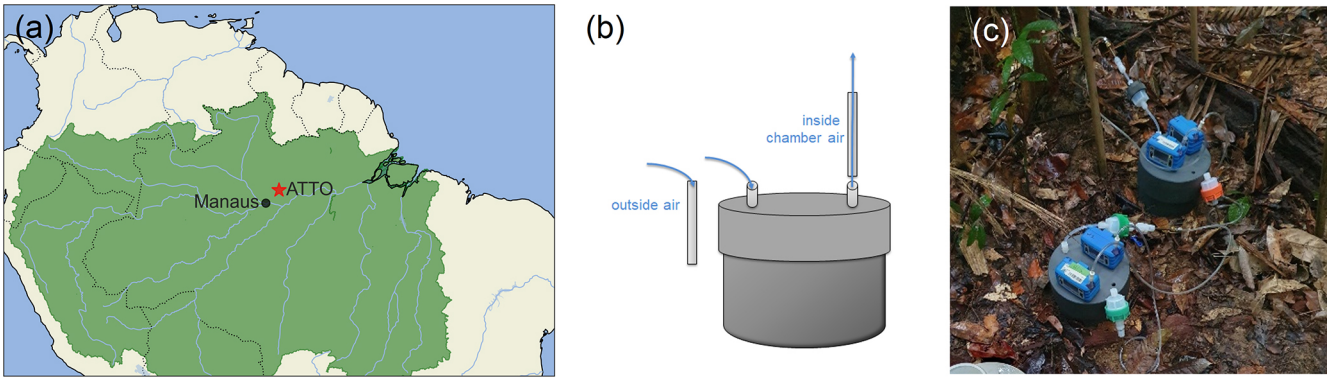

Figure 1. (a) Map of the measurement location with the Amazon Basin watershed region overlaid. (Lehner and Grill, 2013). **(b)** Schematic and **(c)** photo of the soil measurement set-up.

Detection was performed using a Time-of-Flight-Mass Spectrometer (TOF-MS, BenchTOF, MARKES International Ltd., U.K.). The mass range that is recorded by the TOF-MS was set from 40 to 600 m/z. The filament voltage was set between 1.7 and 1.8 V.

The GC-TOF-MS peaks were integrated using chromatography analysis software PARADISe (v 6.1.7 dev) and IDL (Obersteiner et al., 2016). Compounds were quantified using a gas standard calibration mixture and liquid standards injected at 1, 2, 4, 6, 8, and 10 µL in methanol-diluted compound mixtures with a syringe directly onto the sorbent cartridge. Afterwards the cartridge was purged with nitrogen for 10 min to remove the methanol. As liquid standards (−)-limonene (TCI), 3-carene (Merck), (−)-α-cedrene (Sigma-Aldrich), (+)-δ-cadinene (TCI), (+)-cyclosativene (Sigma-Aldrich), (+)-longifolene (PhytoLab), (−)-isolongifolene (Fluka), α-copaene (Biomol), trans-β-ocimene (LGC), (−)-α-phellandrene (Sigma-Aldrich), (−)-α-pinene (thermoscientific), (+)-α-pinene (Acros Organics), (+)-β-pinene (Fluka), sabinene (ChemCruz), β-caryophyllene (Sigma-Aldrich), a-terpinene (Sigma-Aldrich) and γ-terpinene (Sigma-Aldrich) were used in the concentration range between 0.49 to 84.52 nmol L^{-1}. The gas standard mixture contained isoprene, MVK, MACR, tricyclene, (−) and (+)-α-pinene, (−)-β-pinene, (+) and (−)-camphene, sabinene, β-myrcene, (−)-α-phellandrene, (−)-3-carene, α-terpinene, (+)-limonene, γ-terpinene, terpinolene, m- p- and o-cymene, (+) and (−)-linalool, and β-caryophyllene (Apel-Riemer International, USA). When a calibration was performed with calibration gas and liquid standard, the calibration with gas standard was used, as it is more similar to the conditions when filling environmental samples than injecting methanol-diluted compound mixture. For compounds without available gas or liquid standards, quantification was based on the response factor of a compound with the closest mass spectra resemblance. Identifying various SQTs and MTs without standards can be challenging due to their structural similarities, leading to increased uncertainty. β-caryophyllene was used for quantifying uncharacterized SQTs (SQT_unknown), while (−)-β-pinene and (+)-limonene were used for (+)-β-pinene and (−)-limonene, respectively. (+)-camphene and (−)-camphene were used for both detected α-fenchene enantiomers due to their similar structures. Breakthrough was tested by two sorbent cartridges in sequence and concentrations of the calibration gas of up to 10 ppbv with a 6 L sample volume and flow collection rate of 200 mL min^{-1},

which resulted in no detectable targets in the second cartridge. Compounds in the sample chromatogram were identified by matching retention times with those of the standards. Enantiomers elution order of α-pinene, limonene, camphene and β-pinene were ídentified by spiking with enantiomerically pure standards (see Fig. A1 for enantiomer resolution in a chromatogram). Compounds lacking standards were identified by comparing their mass spectra with those in the NIST library (NIST 14 Mass Spectral Library). Peak areas were used to quantify concentrations. The sum of instrumental and sampling procedure variability was assessed by a minimum of five samples with the same amount of standard calibration gas. The standard deviation between these measurements of the same concentration was used as variability in measurement. The standard deviation of the integrated area between these measurements of the same concentration was used as variability in measurement. The values as mean values across all measurement campaigns are reported in percent (as standard deviations divided by the mean values) and were 4 % for isoprene, 13 % for MACR, 10 % for MVK, 7 % for (−)-α-pinene, 12 % for (+)-α-pinene, 6 % for β-myrcene, 9 % for tricyclene, 9 % for (+)-camphene, 6 % for (−)-camphene, 16 % for sabinene, 6 % for α-terpinene, 10 % for (+)-limonene, 6 % for γ-terpinene, and 12 % for β-caryophyllene. For substances with liquid calibration the variability of (−)-α-pinene was used.

2.3 Flux calculations

The VOC fluxes were calculated according to the following formula:

$$F = Q \cdot \frac{C_t - C_0}{A} \quad (1)$$

where F is the flux rate ($\mu mol\, m^{-2}\, h^{-1}$), Q is the flow rate ($200\, mL\, min^{-1}$ equals $0.012\, m^3\, h^{-1}$), A is the chamber area ($0.02956\, m^2$), C_t is the BVOC concentration in the chamber, and C_0 is the BVOC concentration outside the chamber (both in pptv). The flux error was calculated by the variability of the BVOC concentration derived from repeated measurements of a known concentration of analyte and ranged between 3 % for α-pinene and up to 16 % for sabinene as this peak was not separated well. The calibration gas mixture is contributing a systematic error of up to 5 % (as stated by the supplier Apel-Riemer International, USA).

2.4 Soil properties and soil respiration

Soil samples were collected in June 2023 approximately 0.5–1.5 m near spots 1, 2, and 3, where VOCs had been measured in January 2023. Samples were taken using a metal core, and the top 5 cm was retained for analysis. After removing larger roots manually, samples were sieved and stored in plastic bags prior to analysis.

Physicochemical analyses were performed by the Departamento de Ciência do Solo, University of São Paulo. Soil microbial biomass carbon was determined following Vance et al. (1987). Particle density was measured using a pycnometer according to EMBRAPA's Manual de Métodos de Análise de Solo (3rd edition, 2017). Soil texture was assessed using the Bouyoucos hydrometer method (SSSA Book Series 5, 1996). Total nitrogen was extracted by the Kjeldahl method, with electrical conductivity measured via a conductivity meter. Ammonium ($N\text{-}NH_4^+$) and nitrate ($N\text{-}NO_3^-$) concentrations were determined by steam distillation (da Silva, 2009). All procedures followed standard protocols detailed in EMBRAPA manuals.

The chambers contained litter as found at the site, except for one experimental chamber in the dry-to-wet season 2023 and the dry season 2024, where fluxes without litter were investigated and the litter was actively removed. To measure the litter density at the site, litter samples were collected from six spots arranged in a circle of approximately 5 m in the same area as the sampling chambers, ensuring that ongoing flux measurements were not disturbed. The litter was dried in an oven at 60 °C and weighed until no weight change was observable to determine the sample dry weight.

Soil respiration, i.e., soil CO_2 emission flux, was measured using an automated closed dynamic soil flux measuring system consisting of an infrared gas analyzer (LI-870, Licor Inc., Lincoln, NA, USA), an 8-port multiplexer (LI-8250, Licor Inc., Lincoln, NA, USA), and three dynamic soil flux chambers (LI 8200-104 Long-Term Chambers with opaque lids, Licor Inc., Lincoln, NA, USA). The soil flux chambers were placed on PVC collars (ID: 19.4 cm) installed close to spot 1, spot 2, and spot 3 during dry-to-wet season 2023, and close to spot 4 and 5 during dry 2023 and wet season 2024. As done for the manual chamber, the litter layer was removed from spot 3 (Table 1). The soil flux measurement is based on the gas concentration development in the recirculated ambient air within the closed dynamic system once the chamber lid is closed. Each measurement consisted of: 90 s of prepurge (chamber lid open) to flush the lines with the ambient air; 390 s (240 s in January 2023) of closure time; 60 s of post-purge. The soil CO_2 flux was calculated by applying an exponential model to the CO_2 concentration change during chamber closure period (Pugliese et al., 2023). The first 30 s after the chamber closure were omitted due to possible perturbations induced by the chamber closure, and the exponential model was applied to the successive 240 s.

2.5 Meteorological and ozone data

The meteorological data, such as the relative humidity and temperature (measured by a termohygrometer, IAK I-Series (Galltec-Mela)) were taken at 26 m height within the canopy at 80 m walk-up INSTANT tower, which is also located at the ATTO site. Ozone data is from an inlet placed 50 cm above the soil. Ozone concentrations were computed by an Ozone Analyzer (Thermo Environmental Instruments 49i) located in a climatized container at the foot of the tower, that works

by pumping air from the sample inlet, measuring O_3 concentration by a direct relationship with the absorption of UV light.

The soil moisture was measured as soil water content at 10 cm depth close to the INSTANT tower at the ATTO site, at approximately 1 km distance from the measurement site. From the soil water content at 10 cm depth, the water-filled pore space (WFPS) was calculated using the formula $\mathrm{WFPS} = \frac{\theta_v}{n}$ where θ_v represents the volumetric water content and n denotes the total porosity calculated as $n = 1 - \frac{\rho_b}{\rho_p}$. Here ρ_b is the bulk density, assumed to be at $1.18\,\mathrm{g\,cm^{-3}}$ as a mean value for Amazon rainforest soils with similar soil texture (Bernoux et al., 1998) and ρ_p is the particle density of the soil as the mean measured value for the analyzed soil samples.

2.6 Statistical analysis

Statistical analyses were performed using Python (version 3.12.4) with the following packages: numpy (v.2.0.0), pandas (v.2.2.2), matplotlib (v.3.9.1), seaborn (v.0.13.2), statsmodel (v.0.14.5), and scipy (v 1.16.0). Data visualization was conducted using matplotlib and seaborn. Statistical differences were assessed using linear mixed-effect models, because the dataset contains repeated measurements over time from the same soil chambers and ambient sampling points, which violates assumptions of independence of simpler tests. Local time was included as a fixed effect in all models, because we expected a diurnal pattern for the measured VOC fluxes and mixing ratios. To assess seasonal differences in fluxes, a linear mixed-effects model was implemented with season, chamber spot location and local time as fixed effects and the sampling date spot as random effects. Differences between soil spots within a single season were assessed with chamber spot location and local time as fixed effect and the sampling date as random effect. Using the Holm–Bonferroni method, p values were adjusted for multiple comparisons afterwards in both cases. For comparisons of enantiomeric ratios between atmospheric and soil chambers and between seasons, a linear mixed-effect model with fixed effect for local time and a random effect for the sampling date and chamber spot or ambient air sampling location was used. Ratios in both cases were log-transformed prior to analysis to stabilize variance and improve residual normality. To assess the effect size (β coefficient) of environmental parameters on fluxes, mixed-effects models were fitted with fixed effect of local time and adjusting for random effects of measurement date and chamber spot location.. Statistical significance was accepted if $p < 0.05$.

3 Results

3.1 Soil properties

In this study, three separate chambers were set up and sampled in each measured season. Each chamber was placed over soil with distinct characteristics, representing the extremes of soil type and litter coverage in the vicinity of the tower. This strategy allowed us to gauge the range of possible soil fluxes and their drivers, which can be combined with subsequent soil surveys over wider areas to provide realistic regional soil flux estimates. In the first measured season in January 2023, the first chamber (termed spot 1 with litter), was placed in vicinity to a termite nest, on relatively porous soil, with a high soil organic matter content, a natural litter covering, and a correspondingly high CO_2 respiration rate (Table 2). The CO_2 respiration did not show a pronounced diurnal cycle, therefore mean values with standard deviation are reported. In contrast to spot 1, spot 2 and spot 3 had very similar soil physiochemical properties and are more representative of the investigated area. These contrasting sites were deliberately chosen to represent the range of soil properties present in the rainforest. These two soil chambers were placed on less permeable soil, in one chamber the litter was left undisturbed (spot 2 with litter) and in the other the litter was removed (spot 3 without litter), so that the role of litter could be examined. The mean CO_2 flux was around three times lower in Spot 3 with the removed litter layer compared to spot 1 and 2. In contrast to that Spot 1 showed a marked difference in organic content compared to spot 2 and spot 3 (Table 2).

CO_2 respiration was more than three times higher in the chambers with litter content than in the chamber without litter in the dry-to-wet season 2023. Spots 4 and 5, measured in October 2023 and April–May 2023 had similar CO_2 fluxes. Following the dry-to-wet season 2023, the chambers from Spots 1–3 were relocated to new sites to ensure undisturbed soil conditions after sampling for analysis of physicochemical properties (Table 2). During the following three measured seasons, dry 2023, wet 2024, and dry 2024, the chambers were kept at the same locations with spot 1 remaining very close to the same location as before (approximately 0.5 m distance to spot 1 in the dry-to-wet season) and the other two chambers were moved approximately 4–5 m and therefore given the new names spot 4 and spot 5. It is worth noting that the spot 1 chamber was located close (approximately 1 m) to a termite nest in all measured seasons, whose processed wood residues likely contributed to the higher organic content.

Soil physicochemical properties for the three chambers as measured in the dry-to-wet season 2023 are shown in Table 2. At all three spots, the soil was clay-based. The microbial biomass and organic matter content were higher in the spot 1 than in the other two chambers. The removal of litter did not have an impact on the measured soil physiochemical properties.

Table 2. Soil CO_2 respiration rate with standard deviation and physiochemical parameters from the three soil chambers measured in January 2023; soil samples were taken in June 2023.

		Spot 1 with litter	Spot 2 with litter	Spot 3 without litter
CO_2 respiration	[$\mu mol\,m^{-2}\,s^{-1}$]	8.7 ± 0.7	7 ± 1	2.4 ± 0.5
Organic Matter	[$g\,kg^{-1}$]	105.7	74.3	69.9
Colometric Organic Matter	[$g\,dm^{-3}$]	63.3	47.7	44.7
Organic Carbon	[$g\,kg^{-1}$]	61.3	43.1	40.5
Microbial Biomass Carbon	[$mg\,C\,g^{-1}$] of dry soil	1.76	1.49	1.57
N total	[$mg\,kg^{-1}$]	4123	3437	3395
pH	$CaCl_2$	3.53	3.75	3.82
	KCl	3.6	3.78	3.88
Particle Density	[$g\,cm^{-3}$]	2.54	2.58	2.61
Soil texture	Coarse Sand [%]	7	9	9
	Fine Sand [%]	6	3	2
	Total Sand [%]	13	11	11
	Silt [%]	14	23	19
	Clay [%]	73	65	70
Texture Class		clay	clay	clay

The dry weight of litter samples taken at five positions around the areas sampled in the dry-to-wet season 2023 had an average of 9.5 g per chamber area. The five litter samples ranged from 6.1 to 15.2 g, showing significant variability even within a few meters. Nonetheless, based on our visual inspections, we believe the litter amounts contained within the chambers were representative of the location throughout all the sampling periods. When scaled to 1 m^2, the mean litter weights were 322 (207–515) $g\,m^{-2}$.

3.2 Meteorological conditions

At the ATTO site, the mean monthly rainfall during the years 2023–2024 was 59 mm, with the highest rainfall occurring in March 2023 (410 mm) during the wet season and the lowest in August 2023 (23 mm) during the dry season (not shown here). The mean air temperature is higher in the dry seasons, with the highest temperatures in October 2023 reaching up to 37 °C during daytime and dropping to 26 °C at night. Relative humidity in the dry seasons varied from between 80 %–90 % (peaking at 05:00 am) to 45 %–50 % around midday (Fig. 3c). In the wet season 2024 and dry-to-wet 2023, temperatures were cooler and relative humidity (RH) higher; with midday temperature maxima between 28–30 °C (80 % RH) and night time temperature minima between 23–24 °C (100 % RH). Generally, soil temperature peaks later in the day and was less variable spanning from 24–28 °C at 10 cm depth. The soil water content did not show a diel cycle, but rather changed seasonally between 0.17–0.3 $m^3\,m^{-3}$. The calculated water-filled pore space at 10 cm depth was 46 ± 2 % in the dry-to-wet transition season 2023, 28.5 ± 0.4 % in the dry season 2023, 56 ± 4 % in the wet season 2024 and 32.3 ± 0.2 % in the dry season 2024. Photosynthetically active radiation (PAR) (Fig. 3e) is slightly higher during the dry seasons than during wet season. Figure 2 shows the mean diurnal meteorological values of air temperature, soil temperature, relative humidity, soil water content and photosynthetically active radiation (PAR) for the four measurement periods.

3.3 Diurnal and seasonal dynamics of soil terpenoid exchanges

The cartridge measurements taken outside of the chambers were used to determine the ambient mixing ratios of the terpenoids at soil level (15 cm above the ground), while those taken from the chambers were used to derive BVOC soil fluxes. Our measurements revealed distinct patterns in BVOC concentrations and fluxes from the Amazon rainforest soils.

Figure 3 summarizes the mean measured mixing ratios for isoprene, methacrolein (MACR) and methyl vinyl ketone (MVK), total monoterpenes (sabinene, β-myrcene, tricyclene, both enantiomers of α-pinene, 3-carene, both enantiomers of α-fenchene, both enantiomers of camphene, both enantiomers of β-pinene, β-ocimene, both enantiomers of limonene, γ-terpinene, α-terpinene, terpinolene), and total sesquiterpenes (β-caryophyllene, α-copaene, (+)-

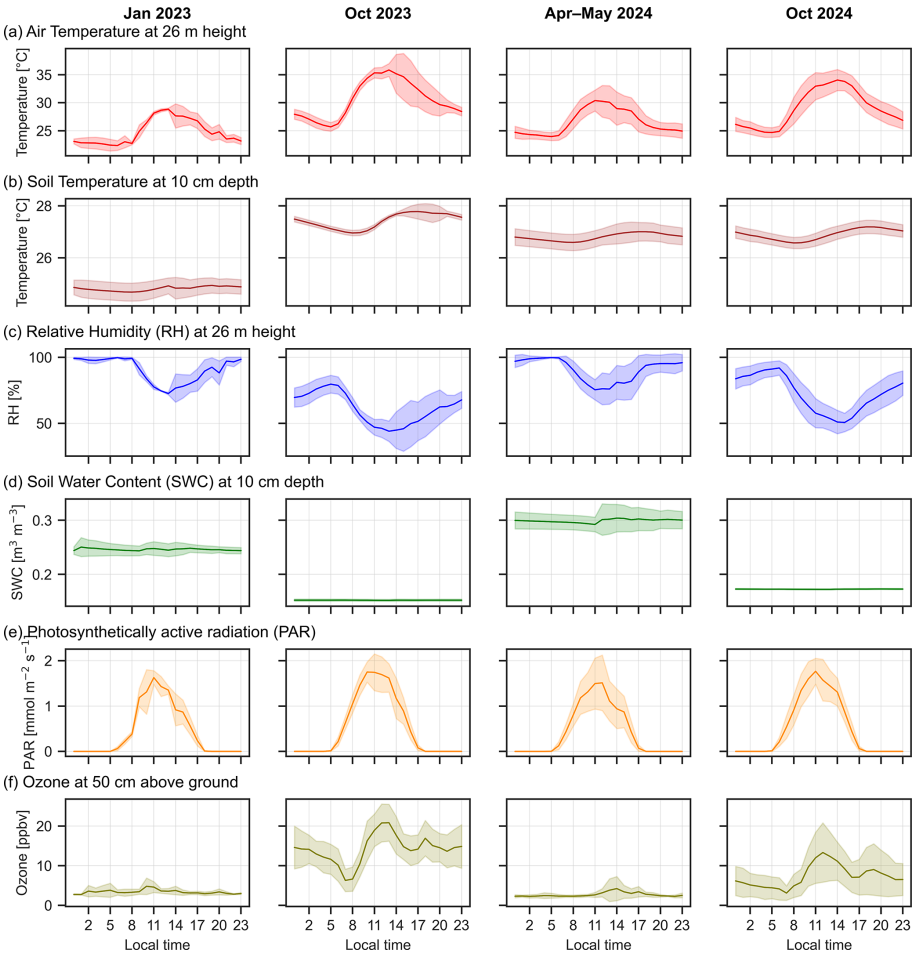

Figure 2. Meteorological data during the measured seasons with **(a)** temperature (red) and **(c)** relative humidity (blue) measured at 26 m at the Instant tower, **(b)** soil temperature (orange) and **(d)** soil water-content (green) measured at 10 cm depth and **(e)** photosynthetically active radiation (PAR) incoming at 81 m at the Instant tower across the four measurement periods in the different seasons. The line represents the mean and shaded area is the standard deviation from the dates of the measurement campaigns specified in Table 1 (number of dates $N = 5$ for January 2023; $N = 14$ for October 2023; $N = 9$ for April–May 2024, $N = 9$ for October 2024).

cyclosativene, (+)-longifolene, (−)-isolongifolene, (−)-α-cedrene and a per campaign differing number of unknown SQTs (good confidence with NIST that they are a SQTs, but with no authentic standard to confirm which exact SQT) at the soil level (outside of the chambers) over the four seasons sampled. The BVOC measurements at soil level showed higher mixing ratios for all terpenoids in the dry seasons (dry 2023 and dry 2024) than in the wet seasons (dry-to-wet 2023 and wet 2024). Isoprene exhibited the largest seasonal change, increasing by almost an order of magnitude from 0.1–1.6 ppbv (wet season) to over 4 ppbv (dry seasons) (Table A1 with mean seasonal values in Appendix A). While isoprene peaked around noon, MTs and SQTs at soil level peaked later in the day in the dry seasons.

Soil level MT and SQT mixing ratios were equivalent to 33 % of the isoprene mixing ratio in the dry season 2023 and 2024, and even at times exceeded isoprene mixing ratio levels in the wet season. SQTs were generally elevated during the dry season 2023; and in both dry season 2023 and dry season 2024, a maximum in SQTs was observed later in the day at 05:00 pm. Diurnal cycles in SQTs were less pronounced in the dry-to-wet and wet seasons.

The net soil fluxes and mean blank values are shown in Fig. 3. The blank values varied in each season, and the number of blanks taken in each campaign is different (Table A2). Therefore, blank values were not subtracted to avoid under- or over-correcting from possibly non-representative blank values. Isoprene and two of its oxidation products methacrolein (MACR) and methyl vinyl ketone (MVK) (Fig. 3) were negative in all four measured seasons, indicating that these species were consistently taken up by the soil. The fluxes of isoprene showed strong seasonal variation, with higher uptake fluxes in the dry season 2023 and 2024 compared to the dry-to-wet and wet seasons (Holm–

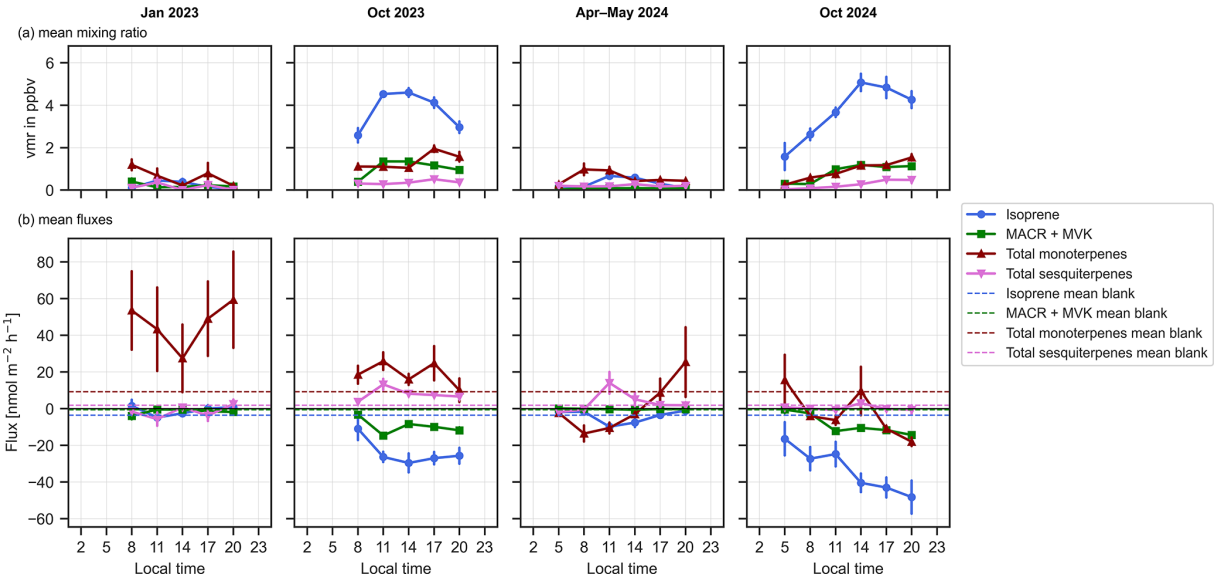

Figure 3. Diurnal curves of the **(a)** mean mixing ratios in ppbv at the soil level and **(b)** mean calculated fluxes in nmol m^{-2} h^{-1} from the soil chambers of isoprene (blue), isoprene oxidation products methacrolein (MACR) and methyl vinyl ketone (MVK), the total monoterpenes (red) and the total sesquiterpenes (pink) over the four measured seasons dry-to-wet 2023, dry 2023, wet 2024 and dry 2024 in the course of a day from 05:00 am to 08:00 pm. Error bars indicate the standard error. Dotted lines represent the mean blank chamber measurements.

Bonferroni adjusted: $p < 0.001$ for comparing October 2024 and $p < 0.01$ for comparing with October 2023; see Table A6).

Unlike isoprene, which was taken up by the soil, MTs and SQTs show remarkable variation between seasons and even between years (Fig. 3). Notably, MTs and SQTs did not display as clear a diurnal cycle as isoprene (Figs. 4 and 5). While MTs and SQTs were predominantly emitted, they were also taken up in many samples in 2024. The emission or uptake was seasonal, time-of-day dependent and mostly specific to the individual soil spot (see Tables A6 and A7 for statistical tests). Interestingly, the SQT emission was significantly higher in the dry season 2023 compared to the dry-to-wet season 2023 ($p < 0.001$) and the dry season 2024 ($p < 0.01$).

3.4 Comparisons of the fluxes from the different soil spots

In this section we examined how the chamber location and associated soil properties (soil spots) influenced the various compounds fluxes over the four seasons. The results are summarized in Fig. 4.

For isoprene, in the dry-to-wet season 2023 and wet season 2024 no significant differences in fluxes were found ($p > 0.05$) (Fig. 4a) between the measured soil chambers. However, in the two dry seasons there was a significantly higher isoprene uptake by spot 1 than spot 5 (Holm–Bonferroni adjusted $p < 0.01$ for dry season 2023 and $p < 0.001$ for dry season 2024) and in the dry season 2024 also in spot 5 than spot 4 (Holm–Bonferroni adjusted $p < 0.001$).

Comparing fluxes of MTs from different soil spots, we note clear monoterpene speciation differences (Fig. 4b). The highest emission rates were observed for soil spot 1 in the dry-to-wet transition season 2023. Here, the flux was significantly higher compared to the other two spots (Holm–Bonferroni adjusted $p < 0.0001$). The flux in spot 1 in both seasons in 2023 was dominated by α-pinene emission, while in the dry season 2024 it was uptaken in the same soil spot. In the other chambers in the dry-to-wet and dry season 2023 α-pinene was uptaken, and ocimene dominated the emission in the dry season 2023. In the wet season 2024 the uptake rates for terpinolene and limonene exceeded those for α-pinene, while in the dry season 2024 α-pinene and limonene dominated the MT uptake fluxes.

The total SQTs flux is dominated by β-caryophyllene and α-copaene, followed by (−)-α-cedrene, (+)-cyclosativene and (+)-δ-cadinene. Some other SQTs could not be identified as no standard was available and the matching factor with the NIST library was high for several different possible SQTs. They are shown as "other sesquiterpenes" (Fig. 4c) The highest observed emission was in the dry season 2023 with values of mean total SQTs emission of 8 ± 2 nmol m^{-2} h^{-1}. In the wet season 2024 and dry season 2024, the mean emission rates were lower at 4 ± 4 and 0.4 ± 0.5 nmol m^{-2} h^{-1}, respectively, and even negative in the dry-to-wet season 2023 at -0.9 ± 0.3 nmol m^{-2} h^{-1}. In the wet and dry season 2024, SQT flux changed between uptake und emission during the day and was soil spot dependent.

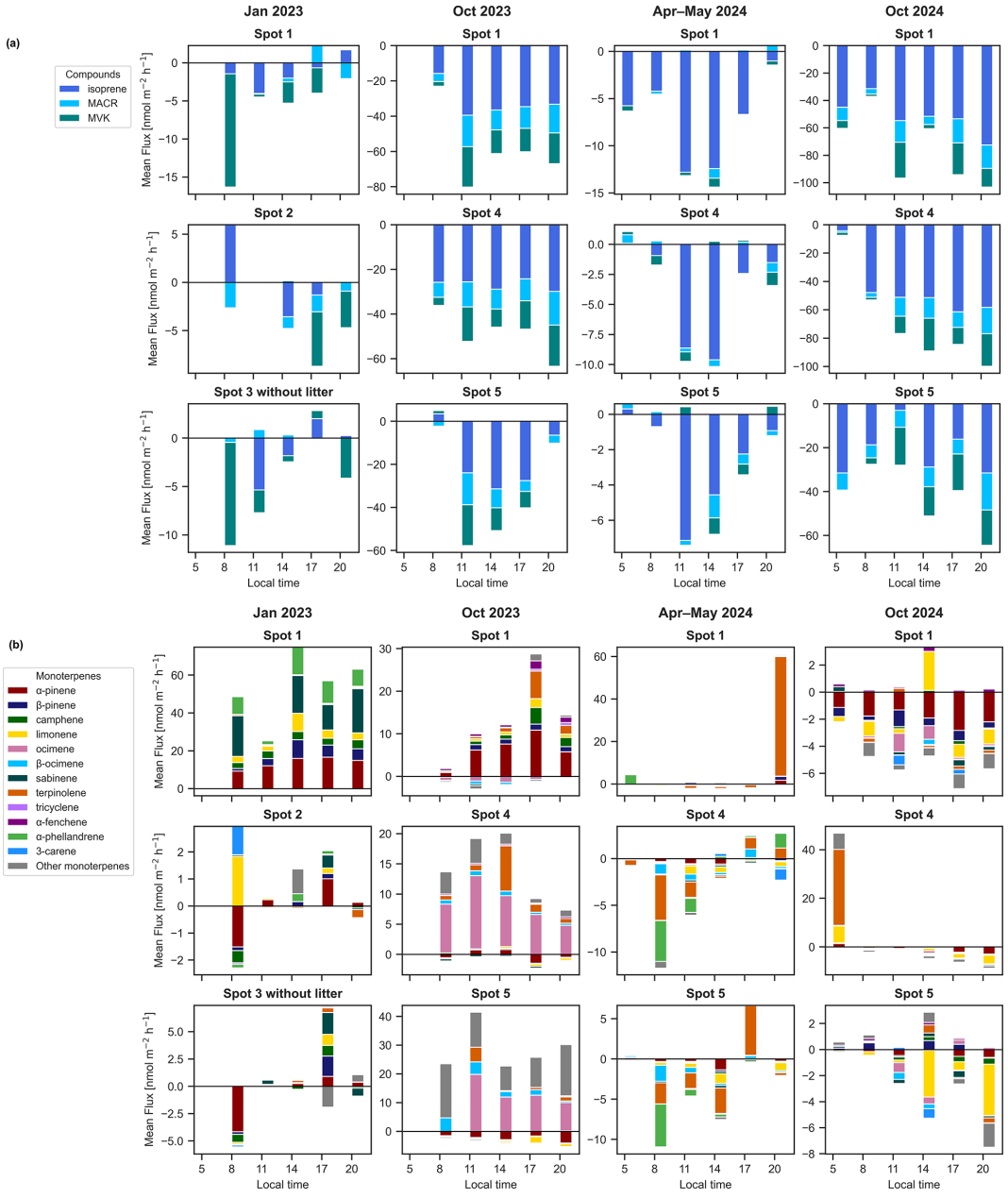
(a)
Jan 2023
Oct 2023
Apr–May 2024
Oct 2024
Spot 1
Spot 2
Spot 3 without litter
Spot 4
Spot 5
Compounds
isoprene
MACR
MVK
Mean Flux [nmol m⁻² h⁻¹]
Local time
(b)
Monoterpenes
α-pinene
β-pinene
camphene
limonene
ocimene
β-ocimene
sabinene
terpinolene
tricyclene
α-fenchene
α-phellandrene
3-carene
Other monoterpenes

Figure 4.

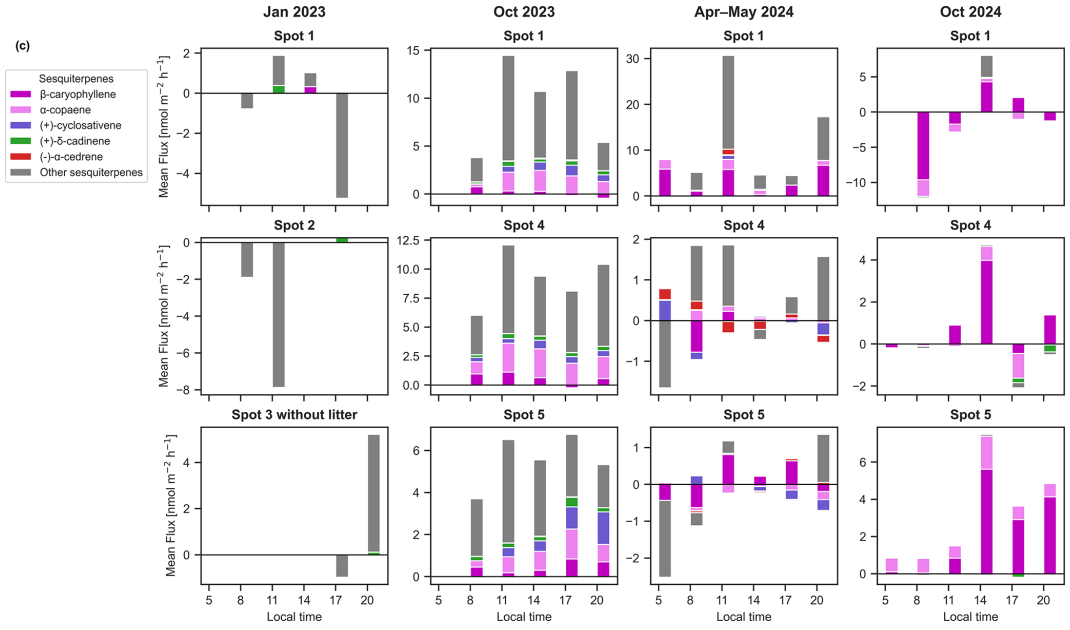

Figure 4. Stacked plots of the mean flux values of the compounds **(a)** isoprene and its oxidation products methacrolein (MACR) and methyl vinyl ketone (MVK), **(b)** monoterpenes and **(c)** sesquiterpenes from the measured chamber spots across seasons except the spots with removed litter layer. Note different *y* axis dimensions.

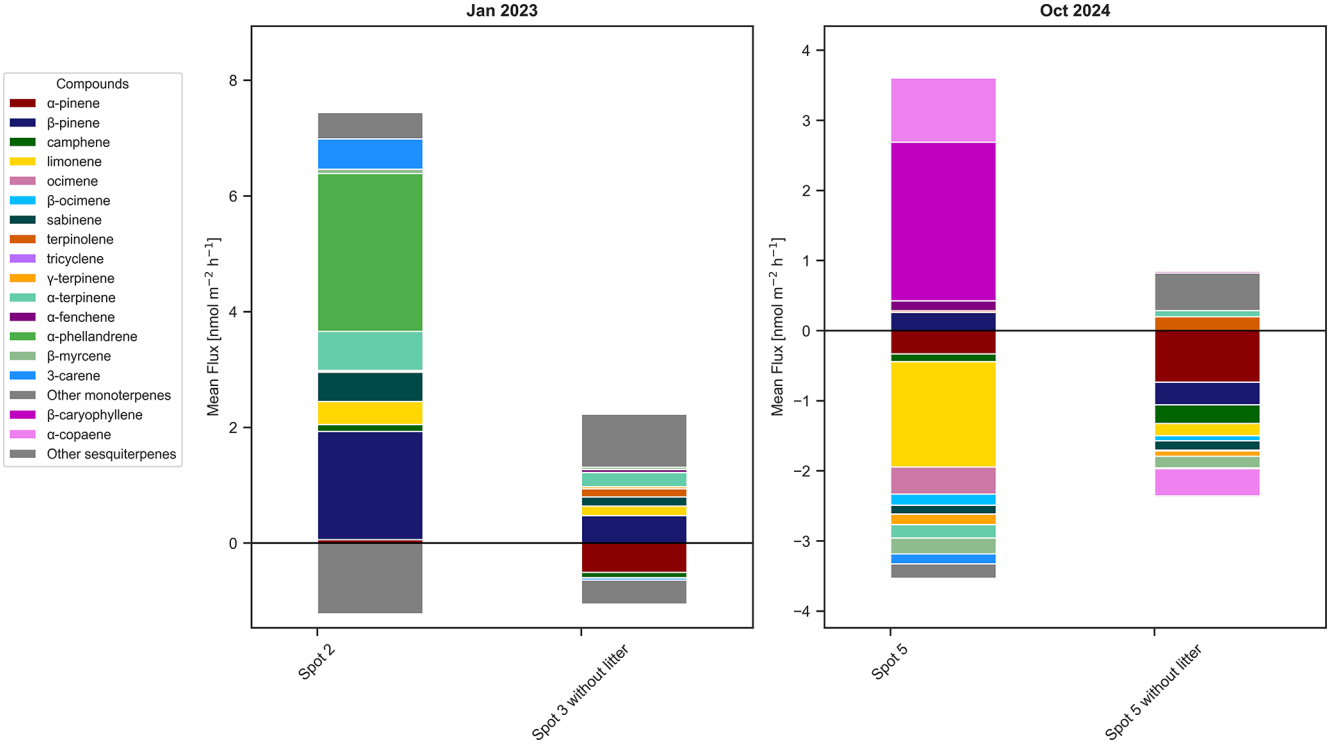

Figure 5. Stacked plots of the mean flux values of monoterpenes and sesquiterpenes showing the difference between the litter layer removed ("without litter") to the one with intact litter layer in the dry-to wet season 2023 for two different spots at the same time and in the dry season 2024 for the same spot before and after litter removal.

Effect of litter removal

When litter was removed from two soil plots, in the two seasons dry-to-wet season 2023 and dry season 2024, no significant difference was found in the fluxes for isoprene and total MTs ($p > 0.05$) when compared to the spot 2 and spot 5 respectively with litter layer. However, there was a notable shift in the terpenoid speciation between the soil chambers with and without litter (Fig. 5). In the dry season 2024, there was an emission of β-pinene, α-copaene and β-caryophyllene in spot 5 with litter and an uptake of those terpenoids when the litter was removed. In contrast, limonene was taken up in both cases, but less with the litter layer intact. Similarly in the dry-to-wet season 2023, β-pinene, α-terpinene, and 3-carene emissions declined with litter removal and α-pinene even shifted from emission to uptake.

3.5 Soil fluxes VS environmental conditions

Isoprene, MVK and MACR have estimated change in flux of -1.2 to $-1.9\,\mathrm{nmol\,m^{-2}\,h^{-1}}$ per ambient atmospheric concentration (Fig. 6) increase in pptv after accounting for diurnal cycles, repeated chamber spot location measurements and dates. Although this result was not significant ($p > 0.05$), it is indicating the uptake rates were higher when the available concentrations in the air above the soil were higher.

Total MTs have an estimated change in flux of more uptake for environmental parameter increasing. The highest effect was found with photosynthetic active radiation (PAR) where the total MT flux decreases an estimated $-31\,\mathrm{nmol\,m^{-2}\,h^{-1}}$ per $\mu\mathrm{mol\,m^{-2}\,s^{-1}}$ ($p < 0.001$) and soil temperature ($p < 0.01$). At the same time ocimene flux is increasing with increased PAR ($p < 0.01$).

Total SQTs did not show a significant result, however β-caryophyllene, α-copaene and (+)-cyclosativene were uptaken more by soil, when air temperature increased ($p < 0.05$, $p < 0.05$ and $p < 0.01$ respectively).

3.6 Atmospheric implications

The emission fluxes from the soil (Flux > 0) were analyzed alongside their lifetimes for the reaction with the hydroxyl radical (OH) and ozone for substances with established reaction constants in the literature (Table B1 in Appendix B shows the used reaction coefficients). The lifetime of each substance emission was calculated with an OH concentration of 1.0×10^6 molecules $\mathrm{cm^{-3}}$ based on estimations of previous studies (Pfannerstill et al., 2021; Ringsdorf et al., 2024) and the measured ozone at 50 cm above the soil, which was in the range of 1.2- 23.5 ppbv.

The mean MT and SQT emission fluxes are shown as measured in Fig. 7, along with the emission fluxes weighted according to their reactivity to OH and O_3. This serves to highlight emissions with greater atmospheric chemistry impact. The importance of the mean emission composition of α-pinene was 28 % in January 2023, but when weighted by its contribution to OH reactivity it was only 16 % and further decreased to 6 % when weighted by its contribution to ozone reactivity. Opposed to this the importance of β-caryophyllene as a reactive sesquiterpene increased from 4 % of total emissions in October 2023, to 5 % contribution to OH reactivity and 52 % responsible for ozone reactivity. The other seasons show similar trends.

3.7 Chirality

The chiral composition of the sampled MTs and SQTs was investigated. Interestingly, for the SQTs found here, only one enantiomer was detected, while for many MTs, both enantiomers were present in the samples.

The (−)-α-pinene was significantly more enriched inside the soil chamber than in the ambient air in the dry-to-wet season 2023 ($p < 0.001$), dry season 2023 ($p < 0.05$), and in the wet season 2024 ($p < 0.01$) (Fig. 8). The ratio of (+)- to (−)-limonene and the ratio of (+)- to (−)-camphene was significantly different in the soil than in the ambient air during the dry 2023, wet 2024, and dry season 2024. The ratio of (+) to (−)-β-pinene was higher in the ambient air than inside the soil chambers in the dry-to-wet 2023, dry 2023, and dry season 2024.

When only comparing the ambient enantiomeric ratios across the season, they are in most cases significantly different from each other (Fig. 8e–h), especially when comparing both dry season 2024 with the dry season 2023 it was significantly different for all chiral MTs, except camphene.

4 Discussion

Our data demonstrate that Amazonian Forest soils act as a sink and source of isoprenoid BVOCs. Isoprene is uptaken in the dry seasons, MTs and SQTs are emitted and uptaken, dependent on season and the local soil spot. Notably, under extreme drought conditions such as those during the 2023 El Niño event, these soils can become sources of highly reactive SQTs.

4.1 Drivers of variation in soil isoprenoid fluxes

4.1.1 Isoprene and the oxidation products MACR and MVK

As shown in Fig. 4, the isoprene mixing ratios followed diurnal cycles with peak levels around noon, which is consistent with light and temperature driven de novo emissions from the canopy above (Guenther et al., 1996; Crutzen et al., 2000; Yáñez-Serrano et al., 2015; Alves et al., 2016; Jardine et al., 2017; Gomes Alves et al., 2023). Isoprene is typically more light-dependent than MTs and SQTs and therefore the observed midday isoprene peak and later MT and SQT maxima

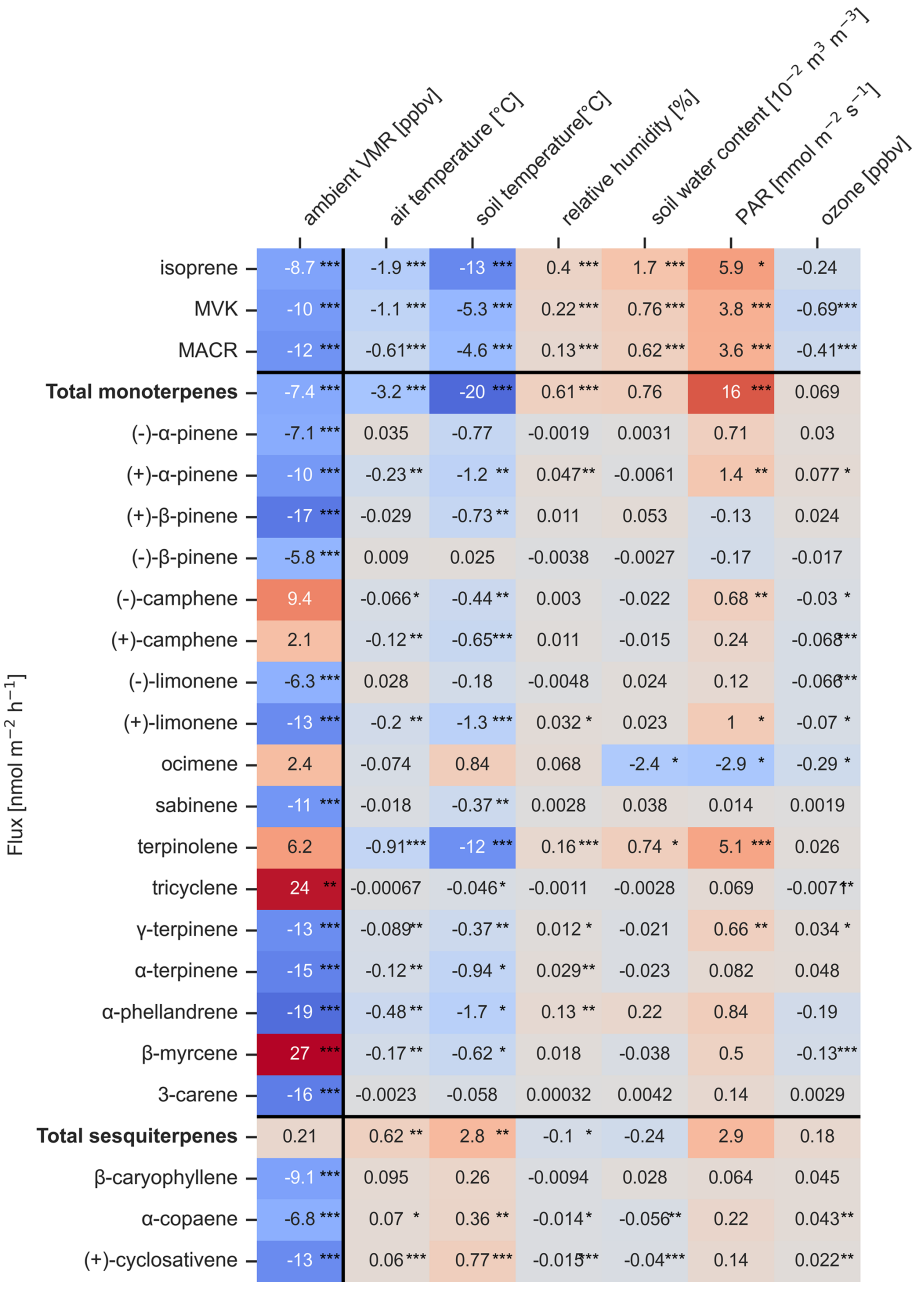

Figure 6. Heatmap of β coefficients from linear mixed-effects models quantifying the change of flux in nmol m^{-2} h^{-1} of measured compounds per unit change in environmental variables, after adjusting for the fixed effect of chamber spot location and random effect for measurement date. Environmental variables are: ambient mixing ratio (VMR) of each compound in ppbv, air temperature at 26 m in °C, incoming photosynthetically active radiation (PAR) at 81 m in mmol m^{-2} s^{-1}, soil temperature in °C and soil water content (scaled by 10^{-2}) at 10 cm depth in 10^{-2} m^3 m^{-3}. Statistical significance of the β coefficients is indicated by asterisks: (*) for $p < 0.05$, (**) for $p < 0.01$ and (***) for $p < 0.001$.

are consistent with previous studies (Guenther et al., 1991; Kuhn et al., 2005; Yañez-Serrano et al., 2018).

In the dry seasons, the soil uptake of isoprene mirrored the ambient diurnal concentration, suggesting it is a key factor in determining the flux. However, no night-time sampling after 08:00 pm or before 05:00 am was performed which could bias the estimates of diel patterns. For isoprene, MACR, and MVK, strong β coefficients between soil fluxes and both ambient mixing ratios and key environmental parameters such as soil water content and temperature (Fig. 7) were negative meaning the uptake rates got higher with higher light intensity and temperature. This hints towards a connection of up-

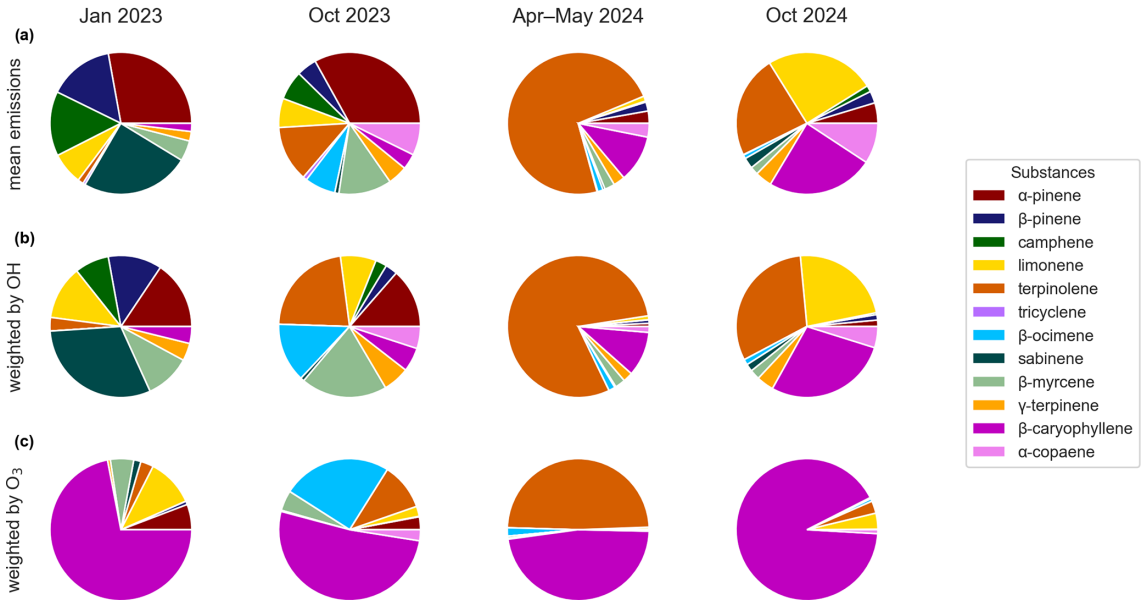

Figure 7. **(a)** Pie charts representing the mean emission fluxes composition. Reactivity impact on atmospheric chemistry towards **(b)** OH radicals and **(c)** Ozone (O_3).

take rates with the simultaneous light- and temperature dependent emission of isoprene. Jiao et al. (2023) found that the size of the BVOC sink in soils was proportional to the atmospheric availability of the compound, indicating that higher uptake rates are driven by higher ambient concentrations.

Laboratory in vitro studies suggest that soil microorganisms like bacterial and fungal taxa consume isoprene (Cleveland and Yavitt, 1997; Gray et al., 2015; Murrell et al., 2020) and use it as a carbon source. At the same time, bacteria can also be emitters of isoprene (Fall and Copley, 2000). Experiments with glass beads and sterilized soils suggest abiotic factors like adsorption and solubility in soil water are playing only a minor role in BVOC fluxes from soil (Cleveland and Yavitt, 1997). Cleveland and Yavitt (1998) reported optimal temperature and soil humidity thresholds for isoprene uptake in temperate forest soils. Accordingly, the pronounced seasonal differences in isoprene uptake observed here likely reflect shifting conditions for the microbial communities which is likely responsible for these processes.

MACR and MVK are the dominant first-generation oxidation products of isoprene (Pierotti et al., 1990), but they can also be directly emitted by plants (Jardine et al., 2012). However, while MACR and MVK play only a minor role in plant' emissions, they have been reported to have a bidirectional flux in and from trees (Fares et al., 2015) and can be absorbed by tree saplings (Tani et al., 2010). Therefore, a net consumption of these compounds by roots and/or microorganisms in the soil is a possible explanation for the observed uptake rates. The processes for the uptake of MACR and MVK may be similar to those of isoprene.

4.1.2 Monoterpenes and sesquiterpenes

MTs showed negative and positive effects on their fluxes by increasing ambient concentrations, PAR and the other environmental variables (Fig. 7), indicating there are different processes responsible for the soil fluxes of each MT. During different seasons, daytime and soil spots, different MT species fluxes were observed (Fig. 5), suggesting very local and seasonally changing processes are at play. The seasonal differences were likely caused by a shift in the microbiome during the transition of an El Niño-influenced year 2023 to the year thereafter, and the different conditions across the different seasons. Roots have also been implicated as sources of MTs from soils (Asensio et al., 2008a), and both plant roots and microbial communities are responsive to climatic variation and drought stress (Bourtsoukidis et al., 2014; Byron et al., 2022; Honeker et al., 2023; Pugliese et al., 2023). So, the roots, as well as the microbiome, could have contributed to the different MT species net fluxes. In a study from similar Amazon rainforest terra firme soil, bacterial communities were observed to shift between dry and wet seasons due to seasonality-related changes in soil nutrient and moisture regimes (Buscardo et al., 2018). In tropical forest soils in Costa Rica bacterial biomass, richness, and enzyme activity peaked at wetter conditions (Kivlin and Hawkes, 2016). Fungal groups in Amazonian soil were observed to shift within 2 months following a nitrogen pulse and come back to their original community microbiome within 5 months (Buscardo et al., 2022). With our measurement we can only make assumptions about the net exchange between the soil-sphere and the atmosphere.

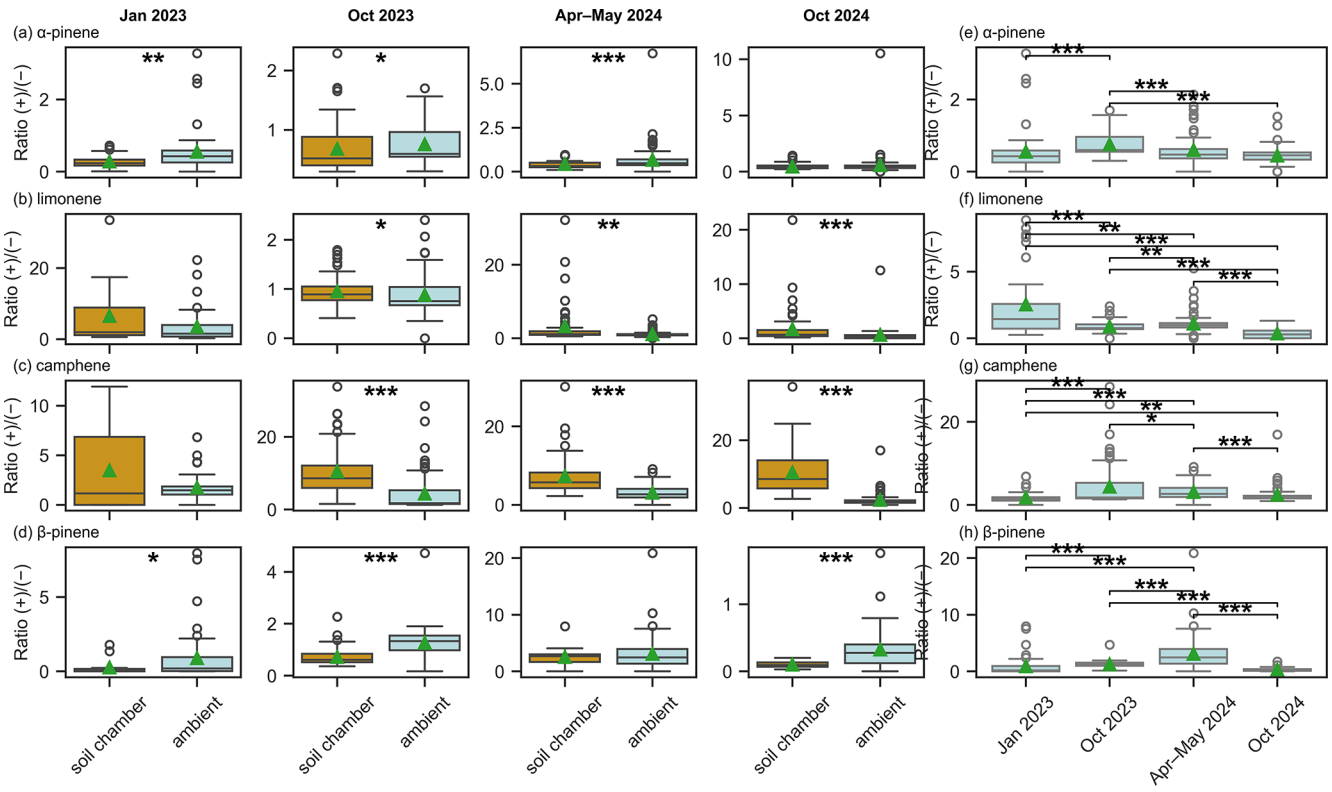

Figure 8. Boxplots show the ratio of the (+)- to (−)-enantiomers for **(a)** α-pinene, **(b)** limonene, **(c)** camphene and **(d)** β-pinene in both ambient air (light blue) and soil chamber air (dark orange) across different seasons. The rightmost panels display the seasonal distribution of ambient air enantiomeric ratios for **(e)** α-pinene, **(f)** limonene, **(g)** camphene and **(h)** β-pinene. The boxes represent 25 % to 75 % of the dataset. Mean values are indicated by green triangles, while the median values are indicated by the central lines. Whiskers indicate the minimum and maximum data points at 1.5 times the interquartile range. Circles represent the outliers. Significance was assessed using linear mixed-effect model accounting for local time as fixed effect; sampling date and chamber spot as random effect. A single asterisk (*) denotes statistically significant differences between groups ($p < 0.05$), double asterisks (**) indicate highly significant differences ($p < 0.01$), and (***) indicate very high significant differences ($p < 0.001$). For improved visualization, in plot **(e)**, two outliers with a ratio of (+)/(−) greater than 5 and in plot **(f)** one outlier with the ratio greater than 10 are not displayed. They are still included in the statistical analysis.

Soil microorganisms, particularly fungi, are known to be significant sources of SQTs (Horváth et al., 2012; Ditengou et al., 2015; Gfeller et al., 2019). A study by Bourtsoukidis et al. (2018) has shown that Amazonian soils can emit SQTs at rates comparable to the plant canopy during the dry season conditions. In contrast, our study did not observe consistent SQT emissions during the two dry seasons of 2023 and 2024. In the El Niño-influenced dry season 2023 the emission of SQT was more pronounced. In the subsequent dry season 2024, SQTs were even partly uptaken by the same soil spots. The extreme dry season in 2023 was characterized by particularly low soil water-filled pore space (WFPS), reaching 30.32 ± 1.27 % at 10 cm depth, closely matching the optimum for SQT emission reported by Bourtsoukidis et al. (2018) at WFPS: 31.3 ± 6.3 %. In contrast, WFPS in the dry season 2024 was higher at 33.64 ± 1.51 %

4.2 Effect of litter

The removal of litter during the dry-to-wet season 2023 and the dry season 2024 in one of the spots each, did not significantly affect the flux of isoprene. This suggests that microorganisms residing in the soil layer beneath the litter are primarily responsible for metabolizing these compounds, while at the same time indicating that litter microbes here have not adapted to isoprene as a carbon source. In contrast, the removal of litter in those two spots did decrease the flux of certain compounds like α-pinene, β-pinene, limonene, camphene, α-copaene and β-caryophyllene. Although this result was not statistically significant ($p > 0.05$ for all before mentioned compounds in both seasons, sample size with litter $n = 23$, without litter $n = 8$) it gives directional evidence towards the role of litter on total soil terpenoid fluxes. The alteration could be attributed to the abiotic degradation of storage pools within the litter material and/or to the production and consumption by microorganisms inhabiting the litter sur-

faces. Abiotic litter emission varies according to decomposition stages as terpenes volatilize from storage pools. As in a tropical forest most plant species are deciduous, storage pool emissions are expected to a lower degree than in litter from coniferous trees (Greenberg et al., 2012; Viros et al., 2021; Isidorov et al., 2024). Previous studies have shown that biotic VOC emissions from litter can be 5 to 10 times higher compared to abiotic processes (Gray et al., 2010), indicating that the microbial community on the litter surfaces plays a significant role in VOC fluxes. Similar findings have been reported in soil terpenoid VOC flux shifts following litter removal in other ecosystems, such as an eucalyptus plantation (Mu et al., 2023), in Boreal forests (Mäki et al., 2017, 2019), and in a Mediterranean forest (Yang et al., 2024). However, very limited information is available for leaf litter volatiles contribution over time (Tang et al., 2019), especially in tropical ecosystems. Litter VOCs were found to have an influence in microbial community structures (McBride et al., 2020) and are known to mediate many microbe–microbe, microbe–plant, and microbe–animal interactions (Bitas et al., 2013; Schmidt et al., 2015; Schulz-Bohm et al., 2017). So, the very local litter structure could be responsible for the different MT and SQTs in the studied soil spots. The highest litter fall rates are usually observed at the end of the dry season and can be increased during an El Niño dry season (Martius et al., 2004; Barlow et al., 2007; Brando et al., 2008), so also the seasonal differences observed for MTs and SQTs could be partly attributed to the litter layer.

4.3 Chirality

In tropical rainforests, the most abundant monoterpene in ambient air is α-pinene, with the $(-)$-enantiomer usually dominating over the $(+)$-enantiomer (Williams et al., 2007; Zannoni et al., 2020; Byron et al., 2022). Recently, experiments using isotopically labelled CO_2 within an enclosed rainforest biome revealed that $(-)$-α-pinene and $(-)$-limonene are, like isoprene, emitted de novo, but also emitted from storage pools, whereas $(+)$-α-pinene and $(+)$-limonene are solely emitted from storage pools (Byron et al., 2022). During the dry-to-wet season 2023, dry season 2023, and the wet season 2024, elevated ratios of $(-)$-α-pinene to $(+)$-α-pinene in soil compared to ambient air suggested a preferential uptake of $(+)$-α-pinene or a preferential emission of $(-)$-α-pinene by the soils. It could be that $(-)$-α-pinene is synthesized de novo by roots or microorganisms in the soil. For β-pinene there seems to be a mechanism at play altering the ratio coming from soils only during the dry seasons and dry-to-wet season, possibly a response to the lower water content in the soil. Camphene and limonene seem to behave similarly to each other and the ratio between soil and ambient is present in all measured seasons except for the dry-to-wet transition season, indicating a consistent difference between the soil enantiomeric fingerprint and the ambient air. So, for these different chiral MT different variables seem to have an influence on the enantiomeric ratio. Chiral monoterpene emissions from plants are known to be tissue-specific, meaning leaves, stem, and belowground emission of enantiomer ratios often differ (Staudt et al., 2019; Daber et al., 2025). So, the roots could be altering the ratio of the chiral enantiomers from the soil, but it is unclear if microbes and fungi also take part. As chiral enantiomers share identical physicochemical properties, abiotic processes cannot explain the discrimination between soil chamber and ambient air ratios. Litter degradation mechanisms could also influence chiral ratios at the soil, as litter fall rates change between seasons (Martius et al., 2004; Barlow et al., 2007; Brando et al., 2008).

As the chiral ratios also change between seasons, but not always between the soil chamber and ambient air, soils are not the only influence on chiral ratios of MTs, above-ground plants must also play an important role. It is known that drought and recovery phases change the chiral ratio of MTs (Byron et al., 2022, 2025), but also mechanical stress or herbivory could impact the ratios, as it is known to alter terpenoid VOC emissions (Holopainen and Gershenzon, 2010; Midzi et al., 2022; Bourtsoukidis et al., 2024).

4.4 Comparison with isoprenoid flux data

4.4.1 Soil fluxes

Here we compare the found soil fluxes with literature values. Very few studies have reported BVOC soil fluxes in tropical rainforests.

Isoprene

The values determined for the uptake flux for isoprene in this study (mean flux of $-19 \pm 7\,\mathrm{nmol\,m^{-2}\,h^{-1}}$ across all seasons) differ from those found in other studies conducted in different ecosystems or an enclosed artificial rainforest environment. For instance, the drought study in an experimental rainforest by Pugliese et al. (2023) and the earlier one by Pegoraro et al. (2006) reported isoprene uptake flux values that are a factor of 1000 higher. We have to note that those studies were carried out in an artificial enclosed rainforest "Biosphere" with no oxidation by OH or O_3 occurring and therefore ambient concentrations of isoprene reach over 200 ppbv, 10 times those found in the natural Amazon ecosystem. This will favor soil bacteria that use ambient isoprene and therefore influence the measured uptake rates. Similarly, a study in an Eucalyptus urophylla plantation forest in subtropical China (Mu et al., 2023) found values for isoprene uptake differing by a factor of 500 to the here found values. Eucalyptus trees are known for their high isoprene emission (Benjamin et al., 1996), and the available isoprene in such plantations makes an increase in isoprene uptake likely. So, these discrepancies can be attributed to the vastly different ecosystem with different conditions than those studied here.

Monoterpenes

The mean flux of total MTs found in this study was $10 \pm 20\,\mathrm{nmol\,m^{-2}\,h^{-1}}$ across all seasons. Other soil flux studies reported values between 174–734 $\mathrm{nmol\,m^{-2}\,h^{-1}}$ for Malaysian Borneo rainforest soil (Drewer et al., 2021) and $76\,\mathrm{nmol\,m^{-2}\,h^{-1}}$ in (unfertilized) soil spots in a tropical rainforest in Guiana (Llusià et al., 2022). Boreal forest showed higher fluxes for MTs from soil in the range of 145–454 $\mathrm{nmol\,m^{-2}\,h^{-1}}$, probably because of storage pool emissions from needle leaf litter (Mäki et al., 2017, 2019).

Conversely, an uptake of MTs of $-73\,\mathrm{nmol\,m^{-2}\,h^{-1}}$ was found in an Eucalyptus urophylla plantation forest in subtropical China (Mu et al., 2023) and a mean uptake rate of $-3\,\mathrm{nmol\,m^{-2}\,h^{-1}}$ in a Mediterranean shrubland (Asensio et al., 2008a). MTs are likely taken up by microorganisms as an energy source and emitted by others and from roots. All of these processes are likely influenced by temperature and soil water content, with each community strain having its optimal conditions for emission or uptake processes.

Sesquiterpenes

The overall mean emission flux for SQTs found here is $4 \pm 2\,\mathrm{nmol\,m^{-2}\,h^{-1}}$. This is low in comparison to another study conducted with soil from the same measurement site but mostly under laboratory conditions (Bourtsoukidis et al., 2018).The fluxes for SQTs identified here are lower by a factor of 10 to 10 000. However, the laboratory study data was derived using BVOC-free air, which was cycled into the chambers and onto soil, generating a maximum potential flux. The air was partially enriched with VOCs from a calibration mixture; however, this cannot reflect the greater chemical diversity of natural conditions as this calibration mixture only contained one MT (α-pinene) and no SQT. As simultaneous soil uptake and emission occurs, the chosen method could be responsible for the observed difference in flux. Another study from a tropical forest in Guyana reported uptake and emission rates for SQT, depending on if they fertilized a soil spot ($122\,\mathrm{nmol\,m^{-2}\,h^{-1}}$) or left it unfertilized ($-323\,\mathrm{nmol\,m^{-2}\,h^{-1}}$) (Llusià et al., 2022). In an eucalyptus plantations also uptake rates of $-30 \pm 16\,\mathrm{nmol\,m^{-2}\,h^{-1}}$ were found (Mu et al., 2023), while in a boreal forest emission rates for SQT of 3–171 $\mathrm{nmol\,m^{-2}\,h^{-1}}$ (Mäki et al., 2017, 2019) and in a tundra 40 000–180 000 $\mathrm{nmol\,m^{-2}\,h^{-1}}$ (Baggesen et al., 2021) were reported. However, we have to note that in the studies with higher emission rates vegetation was inside the used chambers as the soil was naturally covered by plants. So, the soil studies which report SQT fluxes we can compare this study with were mainly performed in vastly different ecosystems, used fertilization treatments or derived under artificial laboratory conditions likely to maximize fluxes.

The higher emission rates of SQT during the dry season 2023 are consistent with the high abundance of sesquiterpenoids measured within the rainforest canopy during the same and similar time periods, which was influenced by El Niño and resulted in severe drought conditions in plants (Pfannerstill et al., 2018; Byron et al., 2025). The largest emissions of SQTs from the soil were noted at the optimal water-filled pore space (WFPS) of approximately 35 % as determined by the model developed by Bourtsoukidis et al. (2018), with a similar value occurring during the extremely dry season 2023.

4.4.2 Context of soil fluxes with canopy and plants fluxes in tropical rainforests

When comparing the uptake rates of isoprene by the soil to the estimated canopy fluxes, they appear rather small. The mean isoprene uptake rate of $-19\,\mathrm{nmol\,m^{-2}\,h^{-1}}$ across all seasons is less than 0.1 % of any reported canopy isoprene flux from tropical rainforests, which are in the range of 11–1007 $\mathrm{\mu mol\,m^{-2}\,h^{-1}}$ (Sarkar et al., 2020; Rizzo et al., 2010; Müller et al., 2008; Karl et al., 2007; Kuhn et al., 2007; Greenberg et al., 2004; Karl et al., 2004; Rinne et al., 2002). However, the isoprene uptake may sustain soil microbes and perform multiple other functions within the soil ecosystem. The actual isoprene used up in soils might be larger when taking into account in the soil produced and emitted isoprene.

The MTs and SQTs fluxes from the soil are also smaller by several orders of magnitude than those reported for the forest canopy. The mean SQT flux of $4 \pm 2\,\mathrm{nmol\,m^{-2}\,h^{-1}}$ found here makes up only a fraction of the estimated SQT canopy flux of 1.7–3.8 $\mathrm{\mu mol\,m^{-2}\,h^{-1}}$ at the site (Alves et al., 2016). However, SQT fluxes are scarce as their lifetimes and concentrations are low, and measurements remain difficult. It likely exerts a disproportionate influence given the high reactivity of SQTs in the atmospheric boundary layer.

The SQT soil flux is also 6 to 500 times smaller compared to cryptogamic species emission rates at the same measurement site that were evaluated per tree surface area: 0.025 to almost 1.96 $\mathrm{\mu mol\,m_{tree}^{-2}\,h^{-1}}$ (Edtbauer et al., 2021).

4.5 Impact on air chemistry

The uptake flux of isoprene by soil is very small compared to the sink via reaction with OH, so it contributes very little to the overall isoprene budget dominated by plants. Also, the emission fluxes of MTs and SQTs from soil are small compared to the canopy fluxes, but the emission of highly reactive species, such as β-caryophyllene, can have an impact on local, near-surface atmospheric chemistry, particularly in relation to particle formation. Our findings indicate that ozone reactivity at the soil level is predominantly driven by emissions of β-caryophyllene (Fig. 8) while α-pinene is less important although it is emitted in higher quantities. Soil emissions could influence the atmospheric oxidative capacity by suppressing oxidants through their reactivity (Dada et al., 2023). This in turn can affect the formation of secondary

organic aerosols (SOAs), a fraction of which will grow to become cloud condensation nuclei and thus impact clouds, weather patterns and climate (Dada et al., 2023; Tripathi et al., 2025). Changes in land use or climate conditions that alter these emissions could, in turn, influence atmospheric composition and climate dynamics. Nevertheless, it is still unclear if these below-canopy emissions have an effect beyond the near-surface processes.

4.6 Limitations of this study and future directions

The study was conducted at three locations on a Terra Firme rainforest plateau, and the samples exhibited significant variability between soil spots. Having only one biological replicate for each of the three soil spots limits possible conclusions to the overall ecosystem soil BVOC flux. Expanding the spatial resolution could provide deeper insights into the overall fluxes of terpenoids at the soil-atmosphere interface in the Amazon rainforest. Measurements were paused during rain to protect the equipment, and while some samples were collected shortly before or after rain events, this may have introduced some bias. Furthermore, logistical constraints limited measurements to between 05:00 am and 08:00 pm potentially omitting nocturnal microbial and abiotic processes.

In the future, actual microbial taxa responsible for certain compounds should be identified. Additionally, isotopic labelling and on-line measurements with a greater time resolution between samples, could further strengthen the understanding of soil BVOC exchange processes, especially in regards to resolving roots and/or microbiome sources.

The storage time of up to two months of the adsorbent cartridges could have resulted in some loss of the higher volatile compounds like isoprene, MACR and MVK. For MTs and SQTs these storage times have been tested previously (Helin et al., 2020). Due to saturation of the instrument (outside linear range) for higher concentrations of isoprene mixing ratios and therefore also fluxes could be underestimated in the dry seasons (Fig. A3).

5 Conclusions

This study highlights the Amazon soil as a dynamic, context-sensitive participant in the regional BVOC budget. The soil-atmosphere exchange of terpenoids and their enantiomers in the Amazon rainforest is strongly connected to season and environmental conditions like temperature and soil moisture. For the uptake of isoprene, MACR, and MVK ambient concentrations and temperature seem to be the primary drivers, while the litter layer here did not have an effect on the consumption of these compounds. MT and SQT net emissions and uptake showed to be governed on the litter layer and season, as well as showing very local differences from spot to spot in the composition of the total flux. Because of the small replication size and the large differences between spots, the effect of the litter layer is exploratory. Enhanced SQT emissions from soil were observed during the El Niño-influenced dry season 2023.

Chiral analysis revealed distinct patterns in the emission and uptake of monoterpene enantiomers, like α-pinene, limonene, camphene and β-pinene, indicating shifts in source contributions, de novo synthesis or possible preferential uptake of one enantiomer over the other. Elevated ratios of $(+)$-β-pinene to $(-)$-β-pinene in soils during the dry season, hint towards a response in the soil to lower soil moisture. Soil processes are influencing the chiral ratio of MTs in the Amazon, but are not the only determining factor as differences in the ratio were also observed in ambient air across seasons.

While soil fluxes of terpenoids are generally much lower than those from the forest canopy, the emission of highly reactive compounds such as SQTs and their oxidation products can impact local atmospheric chemistry and SOA formation (Andreae and Crutzen, 1997; Atkinson, 2000; Williams, 2004; Lelieveld et al., 2008; Tripathi et al., 2025; Bourtsoukidis et al., 2025). These findings underscore the importance of considering soil processes in models of rainforest BVOC emissions, especially in the context of ongoing climate change and increasing frequency of extreme weather events which could enhance SQT emission from soils. By taking up isoprene and the net emission of MTs and SQTs the soil will exert partial control over near-surface ambient atmospheric ozone and OH.

Future research should expand spatial and temporal coverage, integrate microbial community analyses, and further resolve the mechanisms underlying chiral BVOC fluxes. Such efforts are essential for a comprehensive understanding of the Amazon's role in regional and global atmospheric chemistry, especially in the face of climate warming.

Appendix A

Table A1. Mean Retention times, mean measured flux in nmol m^{-2} h^{-1} with standard deviation, mean limit of detection (LOD) across the measurement campaigns in pptv with standard deviation, and mean ambient ratio in pptv with standard deviation of all measured terpenoid substances in each season.

		mean flux [nmol m^{-2} h^{-1}]				ambient vmr [pptv]				
Number of data points		31	70	58	55	Mean LOD [pptv]	33	81	58	54
Substance	mean RT [min]	Jan 2023	Oct 2023	Apr–May 2024	Oct 2024		Jan 2023	Oct 2023	Apr–May 2024	Oct 2024
isoprene	5.50	−1.46 ±4.72	−27.18 ±21.82	−5.00 ±7.06	−35.33 ±26.32	0.81 ±1.68	220.66 ±262.27	3829.13 ±1462.75	356.48 ±448.87	3977.21 ±1922.10
MACR	8.04	−0.58 ±1.25	−10.84 ±7.43	−0.23 ±0.92	−8.63 ±7.07	0.58 ±0.90	92.74 ±78.31	974.02 ±506.21	69.94 ±41.23	820.60 ±476.11
MVK	8.55	−2.94 ±4.68	−11.48 ±8.83	−0.33 ±1.18	−11.34 ±10.30	0.63 ±0.98	303.22 ±291.41	1168.65 ±713.21	95.35 ±53.64	1049.95 ±688.54
sabinene	32.82	2.69 ±6.70	−0.31 ±0.14	−0.14 ±0.21	−0.15 ±0.42	0.51 ±1.10	15.71 ±17.54	30.86 ±9.65	11.81 ±8.42	25.48 ±15.92
tricyclene	33.42	0.09 ±0.21	0.14 ±0.44	0.00 ±0.06	−0.01 ±0.02	0.03 ±0.03	2.88 ±3.10	2.74 ±1.82	1.30 ±0.69	2.24 ±1.28
(−)-α-pinene	33.95	5.63 ±9.86	3.35 ±8.11	−0.30 ±1.56	−1.46 ±1.95	0.21 ±0.68	42.20 ±52.10	312.59 ±144.49	62.43 ±42.52	230.42 ±124.94
(+)-α-pinene	34.44	3.50 ±6.54	1.91 ±5.15	0.05 ±0.61	−0.60 ±1.01	0.18 ±0.58	38.61 ±106.25	222.45 ±168.90	21.48 ±11.59	101.49 ±74.42
3-carene	35.70	0.06 ±0.32	-0.00 ±0.14	-0.19 ±0.64	-0.12 ±0.38	0.18 ±1.18	2.54 ±4.57	2.11 ±6.50	22.85 ±41.13	10.87 ±19.46
(+)-α-fenchene[b]	36.93	0.26 ±0.35	0.88 ±1.86	−0.07 ±0.13	0.19 ±0.19	0.32 ±0.91	0.00 ±0.00	15.07 ±20.76	10.28 ±4.33	2.22 ±3.94
(−)-α-fenchene[b]	37.22	0.17 ±0.13	0.45 ±0.99	−0.01 ±0.04	0.10 ±0.13	0.24 ±1.02	0.00 ±0.00	3.42 ±8.69	3.88 ±1.89	0.85 ±1.08
(+)-camphene	37.63	1.94 ±3.01	0.77 ±2.76	−0.22 ±0.16	−0.35 ±0.55	0.32 ±0.91	10.24 ±22.46	68.85 ±24.63	19.55 ±9.66	55.73 ±23.17
(−)-camphene	38.28	1.49 ±2.63	0.99 ±2.27	−0.00 ±0.08	0.07 ±0.18	0.24 ±1.02	9.86 ±21.10	10.88 ±15.89	3.41 ±2.37	7.44 ±4.91
(+)-β-pinene	39.61	3.33 ±7.38	0.58 ±0.93	0.22 ±1.59	0.12 ±0.24	0.21 ±0.68	2.08 ±4.78	27.08 ±22.66	23.51 ±15.27	14.18 ±8.61
(−)-β-pinene	40.02	1.70 ±2.07	0.41 ±1.18	-0.00 ±0.33	-0.47 ±0.90	0.18 ±0.58	3.95 ±7.88	35.95 ±14.49	11.78 ±14.15	117.78 ±50.05
Ocimene[a]	40.91		6.62 ±7.22		−0.36 ±0.41	0.07 ±0.06		105.92 ±99.78		29.31 ±25.42
(−)-limonene[a]	41.48	1.39 ±2.31	0.27 ±2.38	−0.25 ±0.45	−0.30 ±3.19	0.12 ±0.05	7.07 ±5.79	98.56 ±110.33	27.36 ±24.79	59.94 ±67.64
(+)-limonene	41.87	1.36 ±3.46	0.11 ±1.31	−0.71 ±1.15	−1.18 ±3.98	0.28 ±1.53	10.21 ±8.20	84.53 ±66.76	57.35 ±54.25	91.84 ±212.67
terpinolene	45.32	0.17 ±0.29	2.36 ±6.76	4.13 ±27.40	0.68 ±4.73	0.26 ±0.26	8.72 ±8.41	28.18 ±29.79	91.87 ±102.60	14.46 ±9.11
α-copaene[a]	57.04	0.00 ±0.00	1.54 ±0.89	0.38 ±1.18	−0.06 ±1.59	0.04 ±0.02	0.00 ±0.00	63.81 ±30.85	26.27 ±22.84	115.55 ±116.90
β-caryophyllene	60.78	0.04 ±0.13	0.33 ±0.75	1.90 ±4.82	0.94 ±4.29	1.04 ±6.04	0.00 ±0.00	42.06 ±31.43	24.34 ±51.74	136.66 ±210.52
(+)-cyclosativene[a]	62.65		0.66 ±0.50	−0.02 ±0.39	0.00 ±0.00	0.11 ±0.10		3.41 ±6.67	36.40 ±24.52	0.00 ±0.00
(−)-α-cedrene[a]	63.79	0.00 ±0.01	0.04 ±0.07	0.04 ±0.45	0.00 ±0.00	0.10 ±0.05	0.00 ±0.00	1.51 ±2.20	27.88 ±17.12	0.00 ±0.00
(+)-δ-cadinene[a]	66.24	0.05 ±0.14	0.33 ±0.21	0.01 ±0.05	−0.04 ±0.15	1.00 ±0.71	1.04 ±3.20	14.26 ±6.60	1.96 ±1.31	6.77 ±9.71

	mean flux [pmol m^{-2} s^{-1}]			
Substance	Jan 2023	Oct 2023	Apr–May 2024	Oct 2024
isoprene	−0.48 ± 1.33	−6.76 ± 6.19	−1.29 ± 2.03	−9.81 ± 7.31
MACR	−0.17 ± 0.36	−2.69 ± 2.19	−0.06 ± 0.25	−2.40 ± 1.96
MVK	−0.76 ± 1.27	−2.91 ± 2.50	−0.08 ± 0.33	−3.15 ± 2.86
Total monoterpenes	10.54 ± 14.00	5.44 ± 8.48	0.24 ± 10.26	−0.90 ± 8.44
Total sesquiterpenes	−0.26 ± 1.44	2.21 ± 2.57	1.18 ± 3.88	0.12 ± 1.43

[a] Substance LOD and calibration performed using liquid calibration as described in the method section. [b] Substance only tentatively identified and calibrated to (+)- and (−)-camphene and below a summary of the fluxes of isoprene, MACR, MVK, total monoterpenes, and total sesquiterpenes in SI units pmol m^{-2} s^{-1}.

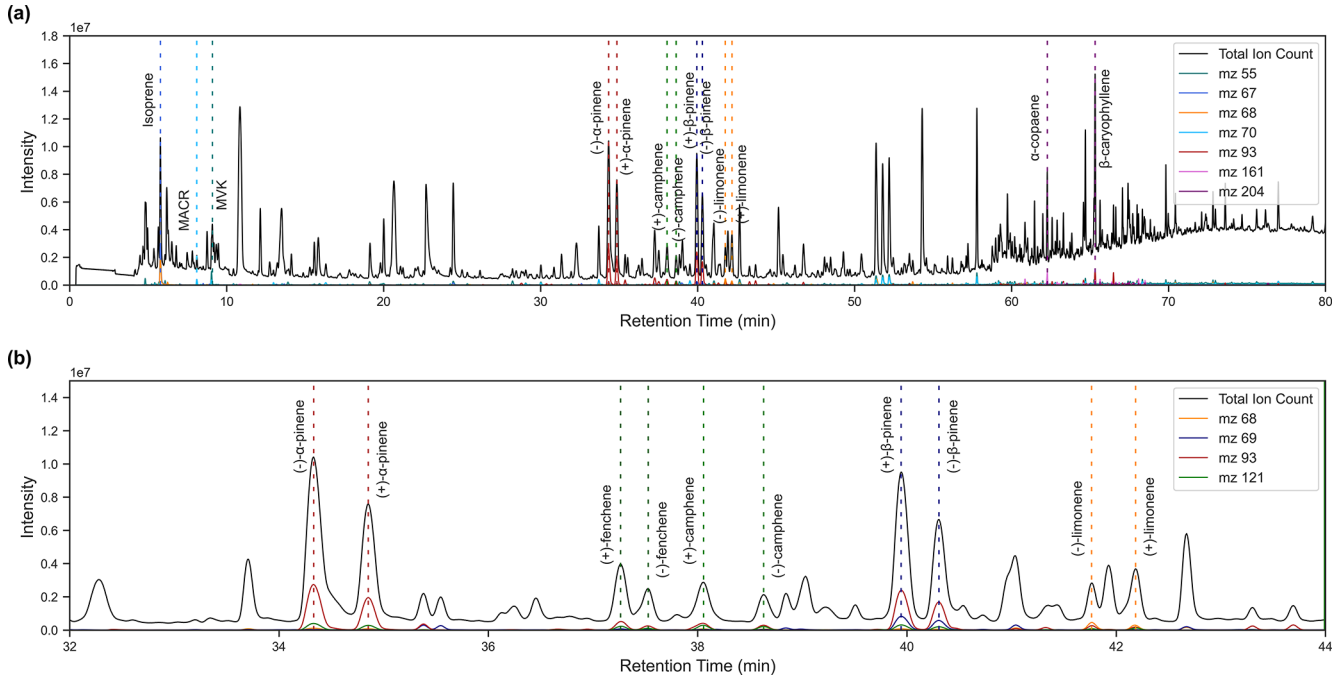

Figure A1. **(a)** Example Chromatogram of a soil chamber sample from October 2023 with annotation of isoprene, MACR, and MVK peaks, the chiral monoterpenes, and the two most prominent sesquiterpenes. **(b)** Zoomed into the chiral monoterpene resolution.

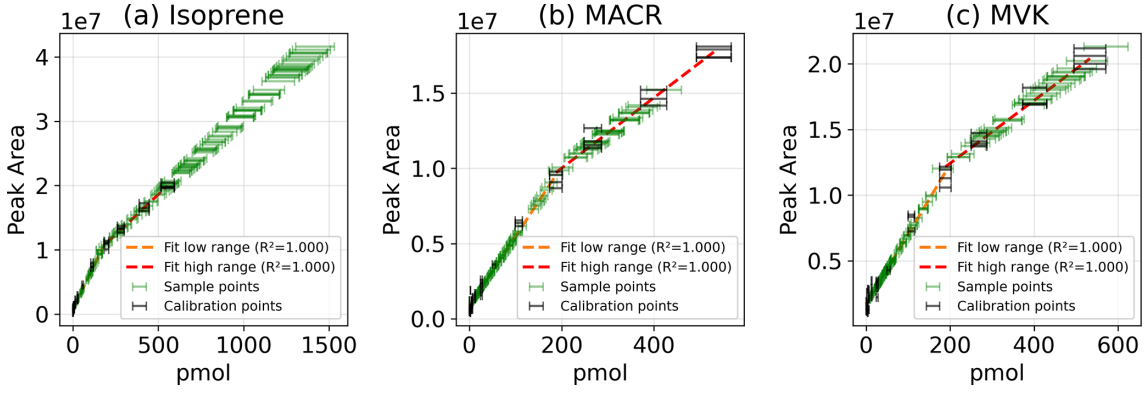

Figure A2. Calibration curve fit of integrated Peak Areas against substance on the cartridge in pmol for **(a)** isoprene, **(b)** MACR, and **(c)** MVK with calibration points with error bars plotted in black, linear fit in the lower range in orange and in the higher range in red, and sample points (from October 2024) in green with error bars.

Table A2. Mean blank measurements from the blank chamber of each substance of the flux in nmol m^{-2} h^{-1} with standard deviation in each season (nan indicates no detection in this campaign; 0 indicates a value ≤ 0.00).

Jan 2023	Oct 2023	Apr–May 2024	Oct 2024	
Number of blank datapoints	2	4	4	11
Substance	flux [nmol m^{-2} h^{-1}]			
isoprene	-6.56 ± 4.30	-0.06 ± 2.33	1.91 ± 9.39	-8.52 ± 15.47
MACR	-1.35 ± 2.16	0.11 ± 3.40	0.03 ± 0.50	-0.66 ± 4.42
MVK	-0.20 ± 0.90	-2.81 ± 6.64	0.28 ± 1.13	0.31 ± 6.47
tricyclene	-0.01 ± 0.00	0.03 ± 0.04	0.01 ± 0.02	-0.01 ± 0.02
(−)-α-pinene	0.17 ± 0.02	1.70 ± 1.66	0.33 ± 1.26	-0.35 ± 1.07
(+)-α-pinene	0.05 ± 0.00	10.85 ± 8.72	-0.01 ± 0.18	-0.38 ± 0.53
sabinene	nan ± nan	0.16 ± 0.13	0.02 ± 0.00	-0.06 ± 0.07
α-phellandrene	0.02 ± 0.02	nan ± nan	$-0.02 \pm$ nan	nan ± nan
3-carene	$0.00 \pm$ nan	-0.00 ± 0.00	nan ± nan	-0.11 ± 0.24
(+)-α-fenchene	nan ± nan	0.10 ± 0.09	$0.08 \pm$ nan	0.07 ± 0.09
(−)-α-fenchene	nan ± nan	0.01 ± 0.01	nan ± nan	0.01 ± 0.01
(+)-camphene	0.00 ± 0.00	0.18 ± 0.21	0.37 ± 0.30	0.01 ± 0.09
(−)-camphene	0.00 ± 0.00	0.28 ± 0.40	0.03 ± 0.05	0.03 ± 0.08
(+)-β-pinene	0.02 ± 0.02	0.24 ± 0.14	$-0.44 \pm$ nan	0.01 ± 0.11
(−)-β-pinene	nan ± nan	0.09 ± 0.08	0.01 ± 0.18	-0.13 ± 0.30
ocimene	nan ± nan	5.56 ± 4.78	nan ± nan	-0.14 ± 0.02
(−)-limonene	0.02 ± 0.01	0.15 ± 0.00	0.08 ± 0.28	0.09 ± 0.55
(+)-limonene	0.02 ± 0.01	3.92 ± 2.80	0.50 ± 0.32	-1.87 ± 5.07
terpinolene	$0.00 \pm$ nan	0.19 ± 0.30	-0.19 ± 0.06	-0.02 ± 0.05
α-copaene	0.00 ± 0.00	0.90 ± 0.95	0.14 ± 0.39	0.19 ± 0.42
(+)-cyclosativene	0.00 ± 0.00	0.25 ± 0.36	0.15 ± 0.55	0.06 ± 0.65
β-caryophyllene	nan ± nan	0.07 ± 0.08	0.30 ± 0.20	0.00 ± 0.00
(−)-α-cedrene	nan ± nan	0.01 ± 0.00	0.21 ± 1.04	0.00 ± 0.00
(+)-δ-cadinene	nan ± nan	0.18 ± 0.18	-0.01 ± 0.00	0.01 ± 0.04

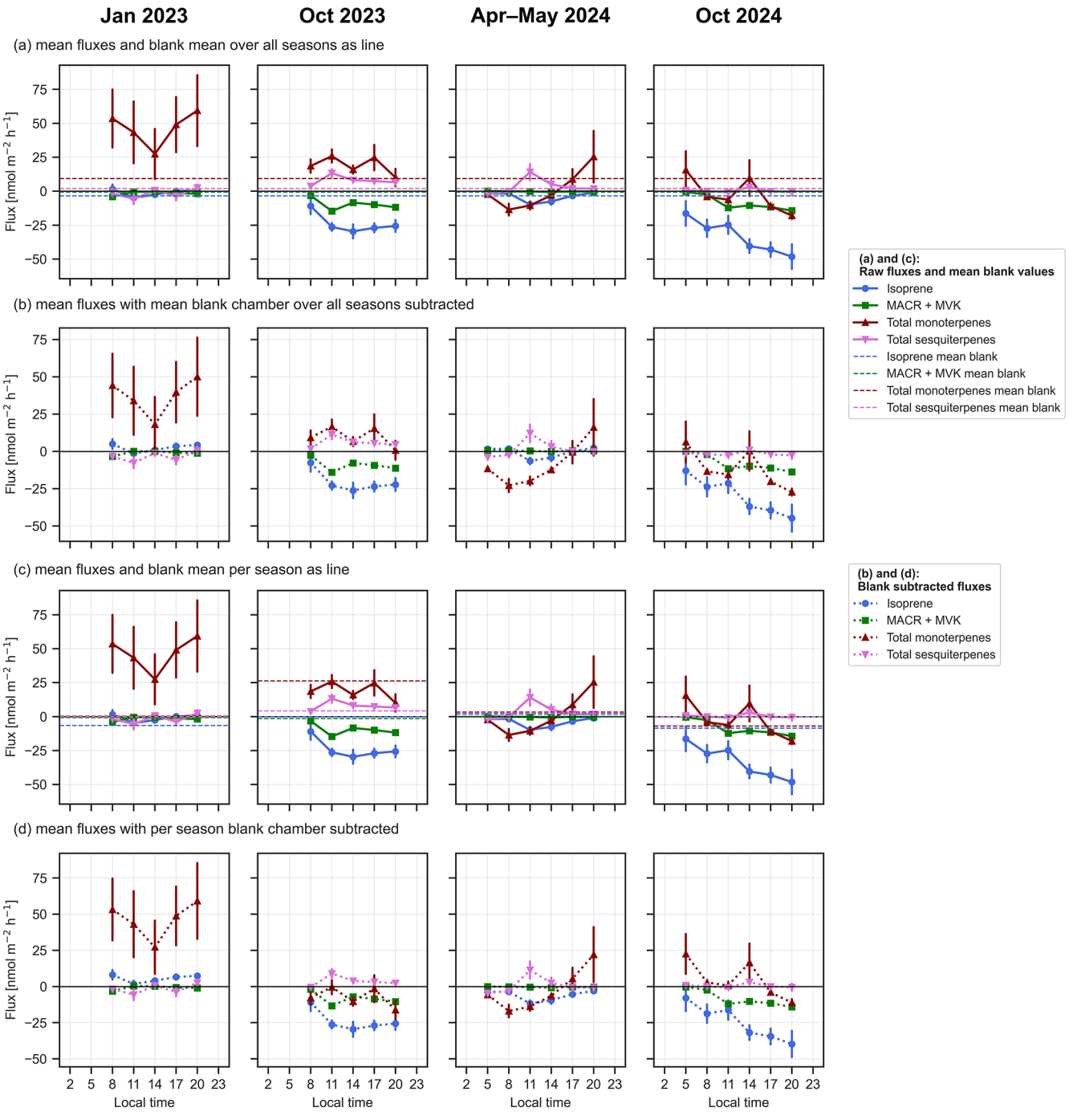

Figure A3. Diurnal curves of the mean calculated fluxes of isoprene (blue), isoprene oxidation products methacrolein (MACR) and methyl vinyl ketone (MVK), the total monoterpenes (red) and the total sesquiterpenes (pink) over the four measured seasons January 2023, October 2023, April–May 2024 and October 2024 in the course of a day from 05:00 am to 08:00 pm with blank values as dotted lines as mean **(a)** over all seasons ($N = 21$) and **(b)** for each season ($N = 2$ for January 2023, $N = 4$ for October 2023, $N = 4$ for April–May 2024, and $N = 11$ for October 2025) and with subtracted blank values from the flux **(b)** over all seasons and **(d)** per season in nmol m^{-2} h^{-1}. Error bars indicate the standard error of the mean.

Table A3. Overview of seasonal differences of the fluxes of isoprene, MACR, MVK, total monoterpenes, and total sesquiterpenes by linear mixed-effect models with the formula "Flux $\sim C$(Season_renamed) + C(Hour) + C(Chamber_spots)" and Date as the random effect; β-coefficients are the estimated change between the baseline season to the compared season (Compared-Baseline) in nmol m^{-2} h^{-1}; 95 % CI is the confidence interval; p value (adj) is the adjusted p value after Holm-Bonferroni correction for multiple comparisons.

Substance	Baseline Season: Compared Season:	Jan 2023 Oct 2023	Jan 2023 Apr–May 2024	Jan 2023 Oct 2024	Oct 2023 Apr–May 2024	Oct 2023 Oct 2024	Apr–May 2024 Oct 2024
isoprene	β-coefficient	−29.029	−4.994	−47.96	20.385	−14.165	−31.634
	95 % CI	−44.6 to −13.458	−10.862–0.873	−67.105 to −28.814	11.632–29.139	−28.297 to −0.032	−44.452 to −18.816
	p value (adj)	7.75×10^{-4}***	0.099	5.47×10^{-6}***	2.00×10^{-5}***	0.099	6.59×10^{-6}***
MACR	β-coefficient	−14.602	0.19	−14.325	10.098	−0.212	−9.586
	95 % CI	−21.059 to −8.145	−0.752–1.132	−21.246 to −7.403	7.113–13.083	−4.651–4.227	−13.348 to −5.824
	p value (adj)	3.72×10^{-5}***	1.000	1.49×10^{-4}***	2.01×10^{-10}***	1.000	2.96×10^{-6}***
MVK	β-coefficient	−8.565	4.524	−10.144	10.802	−2.163	−12.113
	95 % CI	−16.229 to −0.9	2.039–7.01	−21.799–1.511	8.353–13.251	−7.893–3.567	−17.341 to −6.886
	p value (adj)	0.086	0.001**	0.176	3.25×19^{-17}***	0.459	2.79×10^{-5}***
Total MTs	β-coefficient	−72.842	−77.208	−93.614	−12.864	−19.672	−4.739
	95 % CI	−96.934 to −48.751	−107.677 to −46.738	−125.306 to −61.923	−32.544–6.817	−36.833 to −2.512	−29.031–19.553
	p value (adj)	1.86×10^{-8}***	2.73×10^{-6}***	3.53×10^{-8}***	0.400	0.074	0.702
Total SQTs	β-coefficient	11.828	15.698	−1.261	−2.072	−7.71	−4.039
	95 % CI	5.678–17.978	5.988–25.408	−5.912–3.389	−6.445–2.301	−10.996 to −4.424	−8.98–0.902
	p value (adj)	8.17×10^{-4}***	0.006 **	0.706	0.706	2.55×10^{-5}***	0.327

Significance: * $p < 0.05$, ** $p < 0.01$, *** $p < 0.001$.

Table A4. Overview of differences per spot within each season of the fluxes of isoprene, MACR, MVK, total monoterpenes, and total sesquiterpenes by linear mixed-effect models with the formula "Flux $\sim C$(Chamber_spots) + C(Hour)" and Date as random effect; β-coefficients are the estimated change between the baseline spot to the compared spot (Compared-Baseline) in nmol m^{-2} h^{-1}; 95 % CI is the confidence interval; p value (adj) is the adjusted p value after Holm-Bonferroni correction for multiple comparisons.

Substance	Season	Baseline Spot	Compared Spot	β-coefficient	95 % CI	p value (Adj)
isoprene	Jan 2023	Spot 1 ($N = 6$)	Spot 2 ($N = 14$)	0.963	−2.633–4.558	1.000
		Spot 1 ($N = 6$)	Spot 3 without litter ($N = 7$)	1.782	−1.558–5.122	1.000
		Spot 2 ($N = 14$)	Spot 3 without litter ($N = 7$)	0.819	−3.307–4.946	1.000
	Oct 2023	Spot 1 ($N = 52$)	Spot 4 ($N = 24$)	0.102	−9.952–10.157	1.000
		Spot 1 ($N = 52$)	Spot 5 ($N = 25$)	18.133	8.017–28.249	0.012*
		Spot 4 ($N = 24$)	Spot 5 ($N = 25$)	18.031	4.106–31.957	0.223
	Apr–May 2024	Spot 1 ($N = 31$)	Spot 4 ($N = 27$)	2.472	−0.207–5.151	1.000
		Spot 1 ($N = 31$)	Spot 5 ($N = 31$)	3.336	0.807–5.865	0.214
		Spot 4 ($N = 27$)	Spot 5 ($N = 31$)	0.864	−1.714–3.441	1.000
	Oct 2024	Spot 1 ($N = 17$)	Spot 4 ($N = 24$)	−0.26	−10.637–10.116	1.000
		Spot 1 ($N = 17$)	Spot 5 ($N = 25$)	33.689	21.938–45.44	0.000***
		Spot 4 ($N = 24$)	Spot 5 ($N = 25$)	33.949	20.988–46.91	0.000***
		Spot 5 ($N = 25$)	Spot 5 without litter ($N = 12$)	−25.058	−41.86 to −8.256	0.083
MACR	Jan 2023	Spot 1 ($N = 6$)	Spot 2 ($N = 14$)	−1.746	−3.235 to −0.256	0.475
		Spot 1 ($N = 6$)	Spot 3 without litter ($N = 7$)	0.46	−0.944–1.863	1.000
		Spot 2 ($N = 14$)	Spot 3 without litter ($N = 7$)	2.205	0.831–3.58	0.043*
	Oct 2023	Spot 1 ($N = 52$)	Spot 4 ($N = 24$)	2.746	−0.247–5.739	1.000
		Spot 1 ($N = 52$)	Spot 5 ($N = 25$)	5.209	2.207–8.211	0.019*
		Spot 4 ($N = 24$)	Spot 5 ($N = 25$)	2.463	−1.603–6.529	1.000
	Apr–May 2024	Spot 1 ($N = 31$)	Spot 4 ($N = 27$)	0.127	−0.334–0.589	1.000
		Spot 1 ($N = 31$)	Spot 5 ($N = 31$)	−0.293	−0.735–0.149	1.000
		Spot 4 ($N = 27$)	Spot 5 ($N = 31$)	−0.42	−0.894–0.053	1.000
	Oct 2024	Spot 1 ($N = 17$)	Spot 4 ($N = 24$)	2.034	−0.465–4.532	1.000
		Spot 1 ($N = 17$)	Spot 5 ($N = 25$)	5.12	2.465–7.774	0.005**
		Spot 4 ($N = 24$)	Spot 5 ($N = 25$)	3.086	0.501–5.67	0.463
		Spot 5 ($N = 25$)	Spot 5 without litter ($N = 12$)	−2.074	−5.698–1.55	1.000
MVK	Jan 2023	Spot 1 ($N = 6$)	Spot 2 ($N = 14$)	−1.005	−4.237–2.226	1.000
		Spot 1 ($N = 6$)	Spot 3 without litter ($N = 7$)	0.777	−1.827–3.381	1.000
		Spot 2 ($N = 14$)	Spot 3 without litter ($N = 7$)	1.782	−0.872–4.436	1.000
	Oct 2023	Spot 1 ($N = 52$)	Spot 4 ($N = 24$)	3.458	−0.054–6.971	1.000
		Spot 1 ($N = 52$)	Spot 5 ($N = 25$)	5.544	2.017–9.07	0.058
		Spot 4 ($N = 24$)	Spot 5 ($N = 25$)	2.085	−2.549–6.72	1.000
	Apr–May 2024	Spot 1 ($N = 31$)	Spot 4 ($N = 27$)	0.148	−0.407–0.703	1.000
		Spot 1 ($N = 31$)	Spot 5 ($N = 31$)	0.364	−0.289–1.017	1.000
		Spot 4 ($N = 27$)	Spot 5 ($N = 31$)	0.215	−0.417–0.848	1.000
	Oct 2024	Spot 1 ($N = 17$)	Spot 4 ($N = 24$)	1.826	−0.851–4.502	1.000
		Spot 1 ($N = 17$)	Spot 5 ($N = 25$)	5.003	1.703–8.304	0.077
		Spot 4 ($N = 24$)	Spot 5 ($N = 25$)	3.178	−0.075–6.431	1.000
		Spot 5 ($N = 25$)	Spot 5 without litter ($N = 12$)	−7.969	−12.97 to −2.969	0.054
Total MTs	Jan 2023	Spot 1 ($N = 6$)	Spot 2 ($N = 14$)	−104.079	−125.254 to −82.904	0.000***
		Spot 1 ($N = 6$)	Spot 3 without litter ($N = 7$)	−76.622	−98.679 to −54.565	0.000***
		Spot 2 ($N = 14$)	Spot 3 without litter ($N = 7$)	27.457	0.767–54.147	0.963
	Oct 2023	Spot 1 ($N = 52$)	Spot 4 ($N = 24$)	−6.642	−22.658–9.374	1.000
		Spot 1 ($N = 52$)	Spot 5 ($N = 25$)	−12.25	−27.813–3.313	1.000
		Spot 4 ($N = 24$)	Spot 5 ($N = 25$)	−5.608	−27.575–16.36	1.000
	Apr–May 2024	Spot 1 ($N = 31$)	Spot 4 ($N = 27$)	−21.177	−40.488 to −1.866	0.758
		Spot 1 ($N = 31$)	Spot 5 ($N = 31$)	−26.435	−45.807 to −7.063	0.195
		Spot 4 ($N = 27$)	Spot 5 ($N = 31$)	−5.258	−24.104–13.588	1.000
	Oct 2024	Spot 1 ($N = 17$)	Spot 4 ($N = 24$)	−13.325	−29.115–2.465	1.000
		Spot 1 ($N = 17$)	Spot 5 ($N = 25$)	−2.222	−22.226–17.781	1.000
		Spot 4 ($N = 24$)	Spot 5 ($N = 25$)	11.102	−8.798–31.003	1.000
		Spot 5 ($N = 25$)	Spot 5 without litter ($N = 12$)	−6.272	−37.851–25.308	1.000

Table A4. Continued.

Substance	Season	Baseline Spot	Compared Spot	β-coefficient	95 % CI	p value (Adj)
Total SQTs	Jan 2023	Spot 1 ($N = 6$)	Spot 2 ($N = 14$)	−0.849	−6.357–4.659	1.000
		Spot 1 ($N = 6$)	Spot 3 without litter ($N = 7$)	1.137	−3.524–5.798	1.000
		Spot 2 ($N = 14$)	Spot 3 without litter ($N = 7$)	1.986	−3.301–7.274	1.000
	Oct 2023	Spot 1 ($N = 52$)	Spot 4 ($N = 24$)	−2.627	−6.901–1.647	1.000
		Spot 1 ($N = 52$)	Spot 5 ($N = 25$)	−5.737	−10.125 to −1.349	0.229
		Spot 4 ($N = 24$)	Spot 5 ($N = 25$)	−3.11	−8.475–2.255	1.000
	Apr–May 2024	Spot 1 ($N = 31$)	Spot 4 ($N = 27$)	−12.758	−20.51 to −5.007	0.033*
		Spot 1 ($N = 31$)	Spot 5 ($N = 31$)	−12.775	−20.404 to −5.146	0.029*
		Spot 4 ($N = 27$)	Spot 5 ($N = 31$)	−0.016	−7.481–7.448	1.000
	Oct 2024	Spot 1 ($N = 17$)	Spot 4 ($N = 24$)	4.034	1.024–7.043	0.207
		Spot 1 ($N = 17$)	Spot 5 ($N = 25$)	5.974	2.789–9.16	0.007**
		Spot 4 ($N = 24$)	Spot 5 ($N = 25$)	1.941	−1.362–5.244	1.000
		Spot 5 ($N = 25$)	Spot 5 without litter ($N = 12$)	−3.442	−7.927–1.043	1.000

Significance: * $p < 0.05$, ** $p < 0.01$, *** $p < 0.001$.

Appendix B

Table B1. Rate coefficients used for lifetime calculations.

Substance	CAS Number	Rate Coefficient OH (cm^3 $molecule^{-1}$ s^{-1})	Reference	Rate Coefficient Ozone (cm^3 $molecule^{-1}$ s^{-1})	Reference
isoprene	78-79-5	1.01×10^{-10}	Atkinson et al. (2006)	1.29×10^{-17}	Grosjean and Grosjean (1996), Atkinson et al. (1992)
MACR	78-85-3	5.00×10^{-11}	Atkinson (1986)	1.00×10^{-20}	Atkinson et al. (1990)
MVK	78-94-4	1.78×10^{-11}	Chuong and Stevens (2004)	5.40×10^{-18}	Neeb et al. (1998)
α-pinene	80-56-8	5.37×10^{-11}	Atkinson et al. (2006)	9.00×10^{-17}	Atkinson et al. (2006)
β-pinene	127-91-3	7.89×10^{-11}	Atkinson and Arey (2003)	2.10×10^{-17}	Atkinson and Arey (2003)
limonene	5989-27-5	1.61×10^{-10}	Gill and Hites (2002)	6.40×10^{-16}	Atkinson and Arey (2003)
camphene	201-234-8	5.10×10^{-11}	Gaona-Colmán et al. (2017)	5.10×10^{-19}	Gaona-Colmán et al. (2017)
β-myrcene	123-35-3	2.13×10^{-10}	Atkinson (1986)	4.90×10^{-16}	Atkinson et al. (1990)
β-ocimene	3338-55-4	2.50×10^{-10}	Atkinson (1986)	3.15×10^{-15}	Kim et al. (2011)
γ-terpinene	99-85-4	1.77×10^{-10}	Atkinson and Arey (2003)	1.40×10^{-16}	Atkinson and Arey (2003)
α-terpinene	99-86-5	3.60×10^{-10}	Atkinson (1986)	2.10×10^{-14}	Atkinson and Arey (2003)
sabinene	3387-41-5	1.19×10^{-10}	Pang et al. (2023)	3.40×10^{-17}	Pang et al. (2023)
terpinolene	586-62-9	2.30×10^{-10}	Atkinson and Arey (2003)	1.40×10^{-15}	Atkinson et al. (1990)
p-cymene	99-87-6	1.57×10^{-11}	Alarcón et al. (2013)	5.00×10^{-20}	Atkinson et al. (1990)
α-copaene	3856-25-5	9.00×10^{-11}	Atkinson (1986)	2.90×10^{-16}	Estimated (Pollmann et al., 2005)
β-caryophyllene	87-44-5	2.00×10^{-10}	Axel Clausen and Wolkoff (1997)	1.15×10^{-14}	Axel Clausen and Wolkoff (1997), Richters et al. (2015)

Data availability. The data used to support the findings in this study are publicly available on the ATTO data portal and can be accessed with the following DOI: https://doi.org/10.17871/ATTO.612.7.2472 (Schüttler et al., 2025).

Author contributions. JS: Conceptualization, Methodology, Investigation, Visualization, Data curation, Formal analysis, Project administration, Writing – original draft. GP: Conceptualization, Methodology, Investigation, Project administration. JB: Conceptualization, Methodology, Investigation, Project administration. CM: Investigation, Data curation. CQDJ: Investigation, Project administration. HH: Project administration, Supervision. JL: Funding acquisition. JW: Conceptualization, Methodology, Investigation, Funding acquisition, Project administration, Supervision. All authors: Writing – review & editing.

Competing interests. The contact author has declared that none of the authors has any competing interests.

Disclaimer. Publisher's note: Copernicus Publications remains neutral with regard to jurisdictional claims made in the text, published maps, institutional affiliations, or any other geographical representation in this paper. The authors bear the ultimate responsibility for providing appropriate place names. Views expressed in the text are those of the authors and do not necessarily reflect the views of the publisher.

Acknowledgements. For the operation of the ATTO site, we acknowledge the support by the Instituto Nacional de Pesquisas da Amazônia (INPA), the Amazon State University (UEA), the Large-Scale Biosphere-Atmosphere Experiment (LBA), FAPEAM, the Reserva de Desenvolvimento Sustentável do Uatumã (SDS/CEUC/RDS- Uatumã), and the Max Planck Society. Particularly, we would like to thank all colleagues involved in the technical, logistical, and scientific support of the ATTO project. We acknowledge the support by the University of São Paulo (USP) and the Instituto Nacional de Pesquisas da Amazônia (INPA).

During the preparation of this work, the author used perplexity and ChatGPT to improve the readability and language. After using this service, the author reviewed and edited the content as needed and takes full responsibility for the content of the published article.

Financial support. The ATTO project is supported by the Max Planck Society (MPG), the Bundesministerium für Bildung und Forschung (01LB1001A, 01LK1602B, and 01LK2101B), and the Brazilian Ministério da Ciência, Tecnologia e Inovação (01.11.0248.00).

The article processing charges for this open-access publication were covered by the Max Planck Society.

Review statement. This paper was edited by Nicolas Brüggemann and reviewed by Kajsa Roslund and two anonymous referees.

References

Alves, E. G., Jardine, K., Tota, J., Jardine, A., Yãnez-Serrano, A. M., Karl, T., Tavares, J., Nelson, B., Gu, D., Stavrakou, T., Martin, S., Artaxo, P., Manzi, A., and Guenther, A.: Seasonality of isoprenoid emissions from a primary rainforest in central Amazonia, Atmos. Chem. Phys., 16, 3903–3925, https://doi.org/10.5194/acp-16-3903-2016, 2016.

Andreae, M. O. and Crutzen, P. J.: Atmospheric Aerosols: Biogeochemical Sources and Role in Atmospheric Chemistry, Science, 276, 1052–1058, https://doi.org/10.1126/science.276.5315.1052, 1997.

Andreae, M. O., Acevedo, O. C., Araùjo, A., Artaxo, P., Barbosa, C. G. G., Barbosa, H. M. J., Brito, J., Carbone, S., Chi, X., Cintra, B. B. L., da Silva, N. F., Dias, N. L., Dias-Júnior, C. Q., Ditas, F., Ditz, R., Godoi, A. F. L., Godoi, R. H. M., Heimann, M., Hoffmann, T., Kesselmeier, J., Könemann, T., Krüger, M. L., Lavric, J. V., Manzi, A. O., Lopes, A. P., Martins, D. L., Mikhailov, E. F., Moran-Zuloaga, D., Nelson, B. W., Nölscher, A. C., Santos Nogueira, D., Piedade, M. T. F., Pöhlker, C., Pöschl, U., Quesada, C. A., Rizzo, L. V., Ro, C.-U., Ruckteschler, N., Sá, L. D. A., de Oliveira Sá, M., Sales, C. B., dos Santos, R. M. N., Saturno, J., Schöngart, J., Sörgel, M., de Souza, C. M., de Souza, R. A. F., Su, H., Targhetta, N., Tóta, J., Trebs, I., Trumbore, S., van Eijck, A., Walter, D., Wang, Z., Weber, B., Williams, J., Winderlich, J., Wittmann, F., Wolff, S., and Yáñez-Serrano, A. M.: The Amazon Tall Tower Observatory (ATTO): overview of pilot measurements on ecosystem ecology, meteorology, trace gases, and aerosols, Atmos. Chem. Phys., 15, 10723–10776, https://doi.org/10.5194/acp-15-10723-2015, 2015.

Asensio, D., Peñuelas, J., Prieto, P., Estiarte, M., Filella, I., and Llusià, J.: Interannual and seasonal changes in the soil exchange rates of monoterpenes and other VOCs in a Mediterranean shrubland, Eur. J. Soil. Sci., 59, 878–891, https://doi.org/10.1111/j.1365-2389.2008.01057.x, 2008a.

Asensio, D., Owen, S. M., Llusià, J., and Peñuelas, J.: The distribution of volatile isoprenoids in the soil horizons around *Pinus halepensis* trees, Soil. Biol. Biochem., 40, 2937–2947, https://doi.org/10.1016/j.soilbio.2008.08.008, 2008b.

Atkinson, R.: Estimations of OH radical rate constants from H-atom abstraction from C–H and O–H bonds over the temperature range 250–1000 K, Int. J. Chem. Kinet., 18, 555–568, https://doi.org/10.1002/kin.550180506, 1986.

Atkinson, R.: Atmospheric chemistry of VOCs and NOx, Atmos. Environ., 34, 2063–2101, https://doi.org/10.1016/S1352-2310(99)00460-4, 2000.

Atkinson, R. and Arey, J.: Atmospheric Degradation of Volatile Organic Compounds, Chem. Rev., 103, 4605–4638, https://doi.org/10.1021/cr0206420, 2003.

Atkinson, R., Hasegawa, D., and Aschmann, S. M.: Rate constants for the gas-phase reactions of O_3 with a series of monoterpenes and related compounds at 296 ± 2 K, Int. J. Chem. Kinet., 22, 871–887, https://doi.org/10.1002/kin.550220807, 1990.

Atkinson, R., Aschmann, S. M., Arey, J., and Shorees, B.: Formation of OH radicals in the gas phase reactions of O_3

with a series of terpenes, J. Geophys. Res., 97, 6065–6073, https://doi.org/10.1029/92JD00062, 1992.

Atkinson, R., Baulch, D. L., Cox, R. A., Crowley, J. N., Hampson, R. F., Hynes, R. G., Jenkin, M. E., Rossi, M. J., Troe, J., and IUPAC Subcommittee: Evaluated kinetic and photochemical data for atmospheric chemistry: Volume II – gas phase reactions of organic species, Atmos. Chem. Phys., 6, 3625–4055, https://doi.org/10.5194/acp-6-3625-2006, 2006.

Axel Clausen, P. and Wolkoff, P.: Degradation products of Tenax TA formed during sampling and thermal desorption analysis: Indicators of reactive species indoors, Atmos. Environ., 31, 715–725, https://doi.org/10.1016/S1352-2310(96)00230-0, 1997.

Baggesen, N., Li, T., Seco, R., Holst, T., Michelsen, A., and Rinnan, R.: Phenological stage of tundra vegetation controls bidirectional exchange of BVOCs in a climate change experiment on a subarctic heath, Glob. Chang. Biol., 27, 2928–2944, https://doi.org/10.1111/gcb.15596, 2021.

Barlow, J., Gardner, T. A., Ferreira, L. V., and Peres, C. A.: Litter fall and decomposition in primary, secondary and plantation forests in the Brazilian Amazon, Forest Ecol. Manag., 247, 91–97, https://doi.org/10.1016/j.foreco.2007.04.017, 2007.

Barreira, L. M. F., Ylisirniö, A., Pullinen, I., Buchholz, A., Li, Z., Lipp, H., Junninen, H., Hõrrak, U., Noe, S. M., Krasnova, A., Krasnov, D., Kask, K., Talts, E., Niinemets, Ü., Ruiz-Jimenez, J., and Schobesberger, S.: The importance of sesquiterpene oxidation products for secondary organic aerosol formation in a springtime hemiboreal forest, Atmos. Chem. Phys., 21, 11781–11800, https://doi.org/10.5194/acp-21-11781-2021, 2021.

Bellcross, A., Bé, A. G., Geiger, F. M., and Thomson, R. J.: Molecular Chirality and Cloud Activation Potentials of Dimeric α-Pinene Oxidation Products, J. Am. Chem. Soc., 143, 16653–16662, https://doi.org/10.1021/jacs.1c07509, 2021.

Benjamin, M. T., Sudol, M., Bloch, L., and Winer, A. M.: Low-emitting urban forests: A taxonomic methodology for assigning isoprene and monoterpene emission rates, Atmos. Environ., 30, 1437–1452, https://doi.org/10.1016/1352-2310(95)00439-4, 1996.

Bernoux, M., Cerri, C., Arrouays, D., Jolivet, C., and Volkoff, B.: Bulk Densities of Brazilian Amazon Soils Related to Other Soil Properties, Soil Sci. Soc. Am. J., 62, 743–749, https://doi.org/10.2136/sssaj1998.03615995006200030029x, 1998.

Biscaro, T. S., Machado, L. A. T., Giangrande, S. E., and Jensen, M. P.: What drives daily precipitation over the central Amazon? Differences observed between wet and dry seasons, Atmos. Chem. Phys., 21, 6735–6754, https://doi.org/10.5194/acp-21-6735-2021, 2021

Bitas, V., Kim, H.-S., Bennett, J. W., and Kang, S.: Sniffing on Microbes: Diverse Roles of Microbial Volatile Organic Compounds in Plant Health, MPMI, 26, 835–843, https://doi.org/10.1094/MPMI-10-12-0249-CR, 2013.

Bonn, B. and Moortgat, G. K.: Sesquiterpene ozonolysis: Origin of atmospheric new particle formation from biogenic hydrocarbons, Geophys. Res. Lett., 30, https://doi.org/10.1029/2003GL017000, 2003.

Bourtsoukidis, E., Bonn, B., Dittmann, A., Hakola, H., Hellén, H., and Jacobi, S.: Ozone stress as a driving force of sesquiterpene emissions: a suggested parameterisation, Biogeosciences, 9, 4337–4352, https://doi.org/10.5194/bg-9-4337-2012, 2012.

Bourtsoukidis, E., Kawaletz, H., Radacki, D., Schütz, S., Hakola, H., Hellén, H., Noe, S., Mölder, I., Ammer, C., and Bonn, B.: Impact of flooding and drought conditions on the emission of volatile organic compounds of Quercus robur and Prunus serotina, Trees, 28, 193–204, https://doi.org/10.1007/s00468-013-0942-5, 2014.

Bourtsoukidis, E., Behrendt, T., Yañez-Serrano, A. M., Hellén, H., Diamantopoulos, E., Catão, E., Ashworth, K., Pozzer, A., Quesada, C. A., Martins, D. L., Sá, M., Araujo, A., Brito, J., Artaxo, P., Kesselmeier, J., Lelieveld, J., and Williams, J.: Strong sesquiterpene emissions from Amazonian soils, Nat. Commun., 9, 2226, https://doi.org/10.1038/s41467-018-04658-y, 2018.

Bourtsoukidis, E., Pozzer, A., Williams, J., Makowski, D., Peñuelas, J., Matthaios, V. N., Lazoglou, G., Yañez-Serrano, A. M., Lelieveld, J., Ciais, P., Vrekoussis, M., Daskalakis, N., and Sciare, J.: High temperature sensitivity of monoterpene emissions from global vegetation, Commun. Earth Environ., 5, 23, https://doi.org/10.1038/s43247-023-01175-9, 2024.

Bourtsoukidis, E., Guenther, A., Wang, H., Economou, T., Lazoglou, G., Christodoulou, A., Christoudias, T., Nölscher, A., Yañez-Serrano, A. M., and Peñuelas, J.: Environmental Change Is Reshaping the Temperature Sensitivity of Sesquiterpene Emissions and Their Atmospheric Impacts, Global Change Biol., 31, e70258, https://doi.org/10.1111/gcb.70258, 2025.

Brando, P. M., Nepstad, D. C., Davidson, E. A., Trumbore, S. E., Ray, D., and Camargo, P.: Drought effects on litterfall, wood production and belowground carbon cycling in an Amazon forest: results of a throughfall reduction experiment, Philos. Trans. R. Soc. Lond. B. Biol. Sci., 363, 1839–1848, https://doi.org/10.1098/rstb.2007.0031, 2008.

Buscardo, E., Geml, J., Schmidt, S. K., Freitas, H., da Cunha, H. B., and Nagy, L.: Spatio-temporal dynamics of soil bacterial communities as a function of Amazon forest phenology, Sci. Rep., 8, 4382, https://doi.org/10.1038/s41598-018-22380-z, 2018.

Buscardo, E., Geml, J., Schmidt, S. K., Freitas, H., Souza, A. P., Cunha, H. B., and Nagy, L.: Nitrogen pulses increase fungal pathogens in Amazonian lowland tropical rain forests, J. Ecol., 110, 1775–1789, https://doi.org/10.1111/1365-2745.13904, 2022.

Byron, J., Kreuzwieser, J., Purser, G., van Haren, J., Ladd, S. N., Meredith, L. K., Werner, C., and Williams, J.: Chiral monoterpenes reveal forest emission mechanisms and drought responses, Nature, 609, 307–312, https://doi.org/10.1038/s41586-022-05020-5, 2022.

Byron, J., Pugliese, G., A. Monteiro, C. de, Robin, M., Gomes Alves, E., Schuettler, J., Hartmann, S. C., Edtbauer, A., Krumm, B. E., Zannoni, N., Tsokankunku, A., Dias-Junior, C. Q., Quesada, C. A., Harder, H., Bourtsoukidis, E., Lelieveld, J., and Williams, J.: Mirror image molecules expose state of rainforest stress, Commun. Earth Environ., 6, 703, https://doi.org/10.1038/s43247-025-02709-z, 2025.

Chuong, B. and Stevens, P. S.: Measurements of the kinetics of the OH-initiated oxidation of methyl vinyl ketone and methacrolein, Int. J. Chem. Kinet., 36, 12–25, https://doi.org/10.1002/kin.10167, 2004.

Cleveland, C. C. and Yavitt, J. B.: Consumption of atmospheric isoprene in soil, Geophys. Res. Lett., 24, 2379–2382, https://doi.org/10.1029/97GL02451, 1997.

Cleveland, C. C. and Yavitt, J. B.: Microbial Consumption of Atmospheric Isoprene in a Temperate Forest Soil, Appl. Environ. Microbiol., 64, 172–177, https://doi.org/10.1128/AEM.64.1.172-177.1998, 1998.

Crutzen, P. J., Williams, J., Pöschl, U., Hoor, P., Fischer, H., Warneke, C., Holzinger, R., Hansel, A., Lindinger, W., Scheeren, B., and Lelieveld, J.: High spatial and temporal resolution measurements of primary organics and their oxidation products over the tropical forests of Surinam, Atmos. Environ., 34, 1161–1165, https://doi.org/10.1016/S1352-2310(99)00482-3, 2000.

Daber, L. E., Nolte, P., Kreuzwieser, J., Meischner, M., Williams, J., and Werner, C.: Position-specific isotope labelling gives new insights into chiral monoterpene synthesis of Norway spruce (*Picea abies* L.), Environ. Exp. Bot., 238, 106238, https://doi.org/10.1016/j.envexpbot.2025.106238, 2025.

Dada, L., Stolzenburg, D., Simon, M., Fischer, L., Heinritzi, M., Wang, M., Xiao, M., Vogel, A. L., Ahonen, L., Amorim, A., Baalbaki, R., Baccarini, A., Baltensperger, U., Bianchi, F., Daellenbach, K. R., DeVivo, J., Dias, A., Dommen, J., Duplissy, J., Finkenzeller, H., Hansel, A., He, X.-C., Hofbauer, V., Hoyle, C. R., Kangasluoma, J., Kim, C., Kürten, A., Kvashnin, A., Mauldin, R., Makhmutov, V., Marten, R., Mentler, B., Nie, W., Petäjä, T., Quéléver, L. L. J., Saathoff, H., Tauber, C., Tome, A., Molteni, U., Volkamer, R., Wagner, R., Wagner, A. C., Wimmer, D., Winkler, P. M., Yan, C., Zha, Q., Rissanen, M., Gordon, H., Curtius, J., Worsnop, D. R., Lehtipalo, K., Donahue, N. M., Kirkby, J., El Haddad, I., and Kulmala, M.: Role of sesquiterpenes in biogenic new particle formation, Sci. Adv., 9, eadi5297, https://doi.org/10.1126/sciadv.adi5297, 2023.

da Silva, F. C.: Manual De Análises Químicas De Solos, Plantas E Fertilizantes, 2nd edn. rev. e ampl., Embrapa Informação Tecnológica, Brasília, 627 pp., ISBN 978-85-7383-430-7, 2009.

Ditengou, F. A., Müller, A., Rosenkranz, M., Felten, J., Lasok, H., van Doorn, M. M., Legué, V., Palme, K., Schnitzler, J.-P., and Polle, A.: Volatile signalling by sesquiterpenes from ectomycorrhizal fungi reprogrammes root architecture, Nat. Commun., 6, 6279, https://doi.org/10.1038/ncomms7279, 2015.

Drewer, J., Leduning, M. M., Purser, G., Cash, J. M., Sentian, J., and Skiba, U. M.: Monoterpenes from tropical forest and oil palm plantation floor in Malaysian Borneo/Sabah: emission and composition, Environ. Sci. Pollut. Res., 28, 31792–31802, https://doi.org/10.1007/s11356-021-13052-z, 2021.

Edtbauer, A., Pfannerstill, E. Y., Pires Florentino, A. P., Barbosa, C. G. G., Rodriguez-Caballero, E., Zannoni, N., Alves, R. P., Wolff, S., Tsokankunku, A., Aptroot, A., de Oliveira Sá, M., de Araújo, A. C., Sörgel, M., de Oliveira, S. M., Weber, B., and Williams, J.: Cryptogamic organisms are a substantial source and sink for volatile organic compounds in the Amazon region, Commun. Earth Environ., 2, 1–14, https://doi.org/10.1038/s43247-021-00328-y, 2021.

Eerdekens, G., Yassaa, N., Sinha, V., Aalto, P. P., Aufmhoff, H., Arnold, F., Fiedler, V., Kulmala, M., and Williams, J.: VOC measurements within a boreal forest during spring 2005: on the occurrence of elevated monoterpene concentrations during night time intense particle concentration events, Atmos. Chem. Phys., 9, 8331–8350, https://doi.org/10.5194/acp-9-8331-2009, 2009.

El Khawand, M., Crombie, A. T., Johnston, A., Vavlline, D. V., McAuliffe, J. C., Latone, J. A., Primak, Y. A., Lee, S.-K., Whited, G. M., McGenity, T. J., and Murrell, J. C.: Isolation of isoprene degrading bacteria from soils, development of isoA gene probes and identification of the active isoprene-degrading soil community using DNA-stable isotope probing, Environ. Microbiol., 18, 2743–2753, https://doi.org/10.1111/1462-2920.13345, 2016.

Ernle, L., Ringsdorf, M. A., and Williams, J.: Influence of ozone and humidity on PTR-MS and GC-MS VOC measurements with and without a $Na_2S_2O_3$ ozone scrubber, Atmos. Meas. Tech., 16, 1179–1194, https://doi.org/10.5194/amt-16-1179-2023, 2023.

Espinoza, J.-C., Jimenez, J. C., Marengo, J. A., Schongart, J., Ronchail, J., Lavado-Casimiro, W., and Ribeiro, J. V. M.: The new record of drought and warmth in the Amazon in 2023 related to regional and global climatic features, Sci. Rep., 14, 8107, https://doi.org/10.1038/s41598-024-58782-5, 2024.

Fall, R. and Copley, S. D.: Bacterial sources and sinks of isoprene, a reactive atmospheric hydrocarbon, Environ. Microbiol., 2, 123–130, https://doi.org/10.1046/j.1462-2920.2000.00095.x, 2000.

Fares, S., Paoletti, E., Loreto, F., and Brilli, F.: Bidirectional Flux of Methyl Vinyl Ketone and Methacrolein in Trees with Different Isoprenoid Emission under Realistic Ambient Concentrations, Environ. Sci. Technol., 49, 7735–7742, https://doi.org/10.1021/acs.est.5b00673, 2015.

Gao, L., Perrier, S., Iyer, S., Vanoye, L., Fache, F., Claflin, M. S., Kurten, T., and Riva, M.: Unveiling the Role of Chirality in the Oxidation of Monoterpenes, J. Am. Chem. Soc., 147, 28842–28850, https://doi.org/10.1021/jacs.5c06118, 2025.

Gaona-Colmán, E., Blanco, B. M., Barnes, I., Wiesen, P., and Teruel, A. M.: OH- and O_3-initiated atmospheric degradation of camphene: temperature dependent rate coefficients, product yields and mechanisms, RSC Advances, 7, 2733–2744, https://doi.org/10.1039/C6RA26656H, 2017.

Geng, T., Cai, W., Jia, F., and Wu, L.: Decreased ENSO post-2100 in response to formation of a permanent El Niño-like state under greenhouse warming, Nat. Commun., 15, 5810, https://doi.org/10.1038/s41467-024-50156-9, 2024.

Gfeller, V., Huber, M., Förster, C., Huang, W., Köllner, T. G., and Erb, M.: Root volatiles in plant–plant interactions I: High root sesquiterpene release is associated with increased germination and growth of plant neighbours, Plant Cell Environ., 42, 1950–1963, https://doi.org/10.1111/pce.13532, 2019.

Gill, K. J. and Hites, R. A.: Rate Constants for the Gas-Phase Reactions of the Hydroxyl Radical with Isoprene, α- and β-Pinene, and Limonene as a Function of Temperature, J. Phys. Chem. A, 106, 2538–2544, https://doi.org/10.1021/jp013532q, 2002.

Gill, S. S. and Tuteja, N.: Reactive oxygen species and antioxidant machinery in abiotic stress tolerance in crop plants, Plant Physiol. Bioch., 48, 909–930, https://doi.org/10.1016/j.plaphy.2010.08.016, 2010.

Gomes Alves, E., Taylor, T., Robin, M., Pinheiro Oliveira, D., Schietti, J., Duvoisin Júnior, S., Zannoni, N., Williams, J., Hartmann, C., Gonçalves, J. F. C., Schöngart, J., Wittmann, F., and Piedade, M. T. F.: Seasonal shifts in isoprenoid emission composition from three hyperdominant tree species in central Amazonia, Plant Biol., 24, 721–733, https://doi.org/10.1111/plb.13419, 2022.

Gomes Alves, E., Aquino Santana, R., Quaresma Dias-Júnior, C., Botía, S., Taylor, T., Yáñez-Serrano, A. M., Kesselmeier, J., Bourtsoukidis, E., Williams, J., Lembo Silveira de Assis, P. I., Martins, G., de Souza, R., Duvoisin Júnior, S., Guenther, A., Gu, D., Tsokankunku, A., Sörgel, M., Nelson, B., Pinto, D.,

Komiya, S., Martins Rosa, D., Weber, B., Barbosa, C., Robin, M., Feeley, K. J., Duque, A., Londoño Lemos, V., Contreras, M. P., Idarraga, A., López, N., Husby, C., Jestrow, B., and Cely Toro, I. M.: Intra- and interannual changes in isoprene emission from central Amazonia, Atmos. Chem. Phys., 23, 8149–8168, https://doi.org/10.5194/acp-23-8149-2023, 2023.

Gray, C. M., Monson, R. K., and Fierer, N.: Emissions of volatile organic compounds during the decomposition of plant litter, J. Geophys. Res.-Biogeo., 115, https://doi.org/10.1029/2010JG001291, 2010.

Gray, C. M., Helmig, D., and Fierer, N.: Bacteria and fungi associated with isoprene consumption in soil, Elementa: Science of the Anthropocene, 3, 000053, https://doi.org/10.12952/journal.elementa.000053, 2015.

Greenberg, J. P., Guenther, A. B., Pétron, G., Wiedinmyer, C., Vega, O., Gatti, L. V., Tota, J., and Fisch, G.: Biogenic VOC emissions from forested Amazonian landscapes, Glob. Change Biol., 10, 651–662, https://doi.org/10.1111/j.1365-2486.2004.00758.x, 2004.

Greenberg, J. P., Asensio, D., Turnipseed, A., Guenther, A. B., Karl, T., and Gochis, D.: Contribution of leaf and needle litter to whole ecosystem BVOC fluxes, Atmos. Environ., 59, 302–311, https://doi.org/10.1016/j.atmosenv.2012.04.038, 2012.

Grosjean, E. and Grosjean, D.: Rate constants for the gas-phase reaction of ozone with 1, 1-disubstituted alkenes, Int. J. Chem. Kinet., 28, 911–918, https://doi.org/10.1002/(SICI)1097-4601(1996)28:12<911::AID-KIN8>3.0.CO;2-Q, 1996.

Guenther, A., Zimmerman, P., Klinger, L., Greenberg, J., Ennis, C., Davis, K., Pollock, W., Westberg, H., Allwine, G., and Geron, C.: Estimates of regional natural volatile organic compound fluxes from enclosure and ambient measurements, J. Geophys. Res., 101, 1345–1359, https://doi.org/10.1029/95JD03006, 1996.

Guenther, A., Karl, T., Harley, P., Wiedinmyer, C., Palmer, P. I., and Geron, C.: Estimates of global terrestrial isoprene emissions using MEGAN (Model of Emissions of Gases and Aerosols from Nature), Atmos. Chem. Phys., 6, 3181–3210, https://doi.org/10.5194/acp-6-3181-2006, 2006.

Guenther, A. B., Monson, R. K., and Fall, R.: Isoprene and monoterpene emission rate variability: Observations with eucalyptus and emission rate algorithm development, J. Geophys. Res.-Atmos., 96, 10799–10808, https://doi.org/10.1029/91JD00960, 1991.

Guenther, A. B., Jiang, X., Heald, C. L., Sakulyanontvittaya, T., Duhl, T., Emmons, L. K., and Wang, X.: The Model of Emissions of Gases and Aerosols from Nature version 2.1 (MEGAN2.1): an extended and updated framework for modeling biogenic emissions, Geosci. Model Dev., 5, 1471–1492, https://doi.org/10.5194/gmd-5-1471-2012, 2012.

Helin, A., Hakola, H., and Hellén, H.: Optimisation of a thermal desorption-gas chromatography-mass spectrometry method for the analysis of monoterpenes, sesquiterpenes and diterpenes, Atmos. Meas. Tech., 13, 3543–3560, https://doi.org/10.5194/amt-13-3543-2020, 2020.

Herrington, P. R., Craig, J. T., and Sheridan, J. E.: Methyl vinyl ketone: A volatile fungistatic inhibitor from Streptomyces griseoruber, Soil Biol. Biochem., 19, 509–512, https://doi.org/10.1016/0038-0717(87)90092-7, 1987.

Holopainen, J. K. and Gershenzon, J.: Multiple stress factors and the emission of plant VOCs, Trends Plant Sci., 15, 176–184, https://doi.org/10.1016/j.tplants.2010.01.006, 2010.

Honeker, L. K., Pugliese, G., Ingrisch, J., Fudyma, J., Gil-Loaiza, J., Carpenter, E., Singer, E., Hildebrand, G., Shi, L., Hoyt, D. W., Chu, R. K., Toyoda, J., Krechmer, J. E., Claflin, M. S., Ayala-Ortiz, C., Freire-Zapata, V., Pfannerstill, E. Y., Daber, L. E., Meeran, K., Dippold, M. A., Kreuzwieser, J., Williams, J., Ladd, S. N., Werner, C., Tfaily, M. M., and Meredith, L. K.: Drought re-routes soil microbial carbon metabolism towards emission of volatile metabolites in an artificial tropical rainforest, Nat. Microbiol., 8, 1480–1494, https://doi.org/10.1038/s41564-023-01432-9, 2023.

Horváth, E., Hoffer, A., Sebõk, F., Dobolyi, C., Szoboszlay, S., Kriszt, B., and Gelencsér, A.: Experimental evidence for direct sesquiterpene emission from soils, J. Geophys. Res.-Atmos., 117, https://doi.org/10.1029/2012JD017781, 2012.

Huang, H., Ullah, F., Zhou, D.-X., Yi, M., and Zhao, Y.: Mechanisms of ROS Regulation of Plant Development and Stress Responses, Front. Plant Sci., 10, https://doi.org/10.3389/fpls.2019.00800, 2019.

Isaacman-VanWertz, G., Frazier, G., Willison, J., and Faiola, C.: Missing Measurements of Sesquiterpene Ozonolysis Rates and Composition Limit Understanding of Atmospheric Reactivity, Environ. Sci. Technol., 58, 7937–7946, https://doi.org/10.1021/acs.est.3c10348, 2024.

Isidorov, V., Maslowiecka, J., and Sarapultseva, P.: Bidirectional emission of organic compounds by decaying leaf litter of a number of forest-forming tree species in the northern hemisphere, Geoderma, 443, 116812, https://doi.org/10.1016/j.geoderma.2024.116812, 2024.

Jardine, K. J., Monson, R. K., Abrell, L., Saleska, S. R., Arneth, A., Jardine, A., Ishida, F. Y., Serrano, A. M. Y., Artaxo, P., Karl, T., Fares, S., Goldstein, A., Loreto, F., and Huxman, T.: Within-plant isoprene oxidation confirmed by direct emissions of oxidation products methyl vinyl ketone and methacrolein, Global Change Biol., 18, 973–984, https://doi.org/10.1111/j.1365-2486.2011.02610.x, 2012.

Jardine, K. J., Jardine, A. B., Holm, J. A., Lombardozzi, D. L., Negron-Juarez, R. I., Martin, S. T., Beller, H. R., Gimenez, B. O., Higuchi, N., and Chambers, J. Q.: Monoterpene ' *thermometer* ' of tropical forest-atmosphere response to climate warming, Plant Cell Environ., 40, 441–452, https://doi.org/10.1111/pce.12879, 2017.

Jiao, Y., Kramshøj, M., Davie-Martin, C. L., Albers, C. N., and Rinnan, R.: Soil uptake of VOCs exceeds production when VOCs are readily available, Soil Biol. Biochem., 185, 109153, https://doi.org/10.1016/j.soilbio.2023.109153, 2023.

Karl, T., Potosnak, M., Guenther, A., Clark, D., Walker, J., Herrick, J. D., and Geron, C.: Exchange processes of volatile organic compounds above a tropical rain forest: Implications for modeling tropospheric chemistry above dense vegetation, J. Geophys. Res.-Atmos., 109, https://doi.org/10.1029/2004JD004738, 2004.

Karl, T., Guenther, A., Yokelson, R. J., Greenberg, J., Potosnak, M., Blake, D. R., and Artaxo, P.: The tropical forest and fire emissions experiment: Emission, chemistry, and transport of biogenic volatile organic compounds in the lower atmosphere over Amazonia, J. Geophys. Res.-Atmos., 112, https://doi.org/10.1029/2007JD008539, 2007.

Kesselmeier, J. and Staudt, M.: Biogenic Volatile Organic Compounds (VOC): An Overview on Emission,

Physiology and Ecology, J. Atmos. Chem., 33, 23–88, https://doi.org/10.1023/A:1006127516791, 1999.

Kim, D., Stevens, P. S., and Hites, R. A.: Rate Constants for the Gas-Phase Reactions of OH and O_3 with β-Ocimene, β-Myrcene, and α- and β-Farnesene as a Function of Temperature, J. Phys. Chem. A, 115, 500–506, https://doi.org/10.1021/jp111173s, 2011.

Kivimäenpää, M., Markkanen, J.-M., Ghimire, R. P., Holopainen, T., Vuorinen, M., and Holopainen, J. K.: Scots pine provenance affects the emission rate and chemical composition of volatile organic compounds of forest floor, Can. J. For. Res., 48, 1373–1381, https://doi.org/10.1139/cjfr-2018-0049, 2018.

Kivlin, S. N. and Hawkes, C. V.: Temporal and Spatial Variation of Soil Bacteria Richness, Composition, and Function in a Neotropical Rainforest, PLOS ONE, 11, e0159131, https://doi.org/10.1371/journal.pone.0159131, 2016.

Kuhn, U., Dindorf, T., Ammann, C., Rottenberger, S., Guyon, P., Holzinger, R., Ausma, S., Kenntner, T., Helleis, F., and Kesselmeier, J.: Design and field application of an automated cartridge sampler for VOC concentration and flux measurements, J. Environ. Monitor., 7, 568–576, https://doi.org/10.1039/B500057B, 2005.

Kuhn, U., Andreae, M. O., Ammann, C., Araújo, A. C., Brancaleoni, E., Ciccioli, P., Dindorf, T., Frattoni, M., Gatti, L. V., Ganzeveld, L., Kruijt, B., Lelieveld, J., Lloyd, J., Meixner, F. X., Nobre, A. D., Pöschl, U., Spirig, C., Stefani, P., Thielmann, A., Valentini, R., and Kesselmeier, J.: Isoprene and monoterpene fluxes from Central Amazonian rainforest inferred from tower-based and airborne measurements, and implications on the atmospheric chemistry and the local carbon budget, Atmos. Chem. Phys., 7, 2855–2879, https://doi.org/10.5194/acp-7-2855-2007, 2007.

Lehner, B. and Grill, G.: Global river hydrography and network routing: baseline data and new approaches to study the world's large river systems, Hydrol. Process., 27, 2171–2186, https://doi.org/10.1002/hyp.9740, 2013.

Lelieveld, J., Butler, T. M., Crowley, J. N., Dillon, T. J., Fischer, H., Ganzeveld, L., Harder, H., Lawrence, M. G., Martinez, M., Taraborrelli, D., and Williams, J.: Atmospheric oxidation capacity sustained by a tropical forest, Nature, 452, 737–740, https://doi.org/10.1038/nature06870, 2008.

Llusià, J., Asensio, D., Sardans, J., Filella, I., Peguero, G., Grau, O., Ogaya, R., Gargallo-Garriga, A., Verryckt, L. T., Van Langenhove, L., Brechet, L. M., Courtois, E., Stahl, C., Janssens, I. A., and Peñuelas, J.: Contrasting nitrogen and phosphorus fertilization effects on soil terpene exchanges in a tropical forest, Sci. Total Environ., 802, 149769, https://doi.org/10.1016/j.scitotenv.2021.149769, 2022.

Mäki, M., Heinonsalo, J., Hellén, H., and Bäck, J.: Contribution of understorey vegetation and soil processes to boreal forest isoprenoid exchange, Biogeosciences, 14, 1055–1073, https://doi.org/10.5194/bg-14-1055-2017, 2017.

Mäki, M., Aaltonen, H., Heinonsalo, J., Hellén, H., Pumpanen, J., and Bäck, J.: Boreal forest soil is a significant and diverse source of volatile organic compounds, Plant Soil, 441, 89–110, https://doi.org/10.1007/s11104-019-04092-z, 2019.

Martius, C., Höfer, H., Garcia, M. V. B., Römbke, J., and Hanagarth, W.: Litter fall, litter stocks and decomposition rates in rainforest and agroforestry sites in central Amazonia, Nutr. Cycl. Agroecosys., 68, 137–154, https://doi.org/10.1023/B:FRES.0000017468.76807.50, 2004.

McBride, S. G., Choudoir, M., Fierer, N., and Strickland, M. S.: Volatile organic compounds from leaf litter decomposition alter soil microbial communities and carbon dynamics, Ecology, 101, e03130, https://doi.org/10.1002/ecy.3130, 2020.

McGenity, T. J., Crombie, A. T., and Murrell, J. C.: Microbial cycling of isoprene, the most abundantly produced biological volatile organic compound on Earth, ISME J., 12, 931–941, https://doi.org/10.1038/s41396-018-0072-6, 2018.

Midzi, J., Jeffery, D. W., Baumann, U., Rogiers, S., Tyerman, S. D., and Pagay, V.: Stress-Induced Volatile Emissions and Signalling in Inter-Plant Communication, Plants, 11, 2566, https://doi.org/10.3390/plants11192566, 2022.

Mu, Z., Zeng, J., Zhang, Y., Song, W., Pang, W., Yi, Z., Asensio, D., Llusià, J., Peñuelas, J., and Wang, X.: Soil uptake of isoprenoids in a Eucalyptus urophylla plantation forest in subtropical China, Front. For. Glob. Change, 6, https://doi.org/10.3389/ffgc.2023.1260327, 2023.

Müller, J.-F., Stavrakou, T., Wallens, S., De Smedt, I., Van Roozendael, M., Potosnak, M. J., Rinne, J., Munger, B., Goldstein, A., and Guenther, A. B.: Global isoprene emissions estimated using MEGAN, ECMWF analyses and a detailed canopy environment model, Atmos. Chem. Phys., 8, 1329–1341, https://doi.org/10.5194/acp-8-1329-2008, 2008.

Murrell, J. C., McGenity, T. J., and Crombie, A. T.: Microbial metabolism of isoprene: a much-neglected climate-active gas, Microbiol.-UK, 166, 600–613, https://doi.org/10.1099/mic.0.000931, 2020.

Neeb, P., Kolloff, A., Koch, S., and Moortgat, G. K.: Rate constants for the reactions of methylvinyl ketone, methacrolein, methacrylic acid, and acrylic acid with ozone, Int. J. Chem. Kinet., 30, 769–776, https://doi.org/10.1002/(SICI)1097-4601(1998)30:10<769::AID-KIN9>3.0.CO;2-T, 1998.

NOAA's Climate Prediction Center: https://www.cpc.ncep.noaa.gov/products/analysis_monitoring/ensostuff/ONI_v5.php, last access: 7 January 2026.

Norin, T.: Chiral chemodiversity and its role for biological activity. Some observations from studies on insect/insect and insect/plant relationships, Pure Appl. Chem., 68, 2043–2049, https://doi.org/10.1351/pac199668112043, 1996.

Obersteiner, F., Bönisch, H., and Engel, A.: An automated gas chromatography time-of-flight mass spectrometry instrument for the quantitative analysis of halocarbons in air, Atmos. Meas. Tech., 9, 179–194, https://doi.org/10.5194/amt-9-179-2016, 2016.

Owen, S. M., Clark, S., Pompe, M., and Semple, K. T.: Biogenic volatile organic compounds as potential carbon sources for microbial communities in soil from the rhizosphere of Populus tremula, FEMS Microbiol. Lett., 268, 34–39, https://doi.org/10.1111/j.1574-6968.2006.00602.x, 2007.

Pang, J. Y. S., Berg, F., Novelli, A., Bohn, B., Färber, M., Carlsson, P. T. M., Dubus, R., Gkatzelis, G. I., Rohrer, F., Wedel, S., Wahner, A., and Fuchs, H.: Atmospheric photooxidation and ozonolysis of sabinene: reaction rate coefficients, product yields, and chemical budget of radicals, Atmos. Chem. Phys., 23, 12631–12649, https://doi.org/10.5194/acp-23-12631-2023, 2023.

Pegoraro, E., Rey, A., Abrell, L., Haren, J. V., and Lin, G.: Drought effect on isoprene production and consumption in Bio-

sphere 2 tropical rainforest, Glob. Change Biol., 12, 456–469, https://doi.org/10.1111/j.1365-2486.2006.01112.x, 2006.

Peñuelas, J., Asensio, D., Tholl, D., Wenke, K., Rosenkranz, M., Piechulla, B., and Schnitzler, J. p.: Biogenic volatile emissions from the soil, Plant Cell Environ., 37, 1866–1891, https://doi.org/10.1111/pce.12340, 2014.

Pfannerstill, E. Y., Nölscher, A. C., Yáñez-Serrano, A. M., Bourtsoukidis, E., Keßel, S., Janssen, R. H. H., Tsokankunku, A., Wolff, S., Sörgel, M., Sá, M. O., Araújo, A., Walter, D., Lavriè, J., Dias-Júnior, C. Q., Kesselmeier, J., and Williams, J.: Total OH Reactivity Changes Over the Amazon Rainforest During an El Niño Event, Front. For. Glob. Change, 1, https://doi.org/10.3389/ffgc.2018.00012, 2018.

Pfannerstill, E. Y., Reijrink, N. G., Edtbauer, A., Ringsdorf, A., Zannoni, N., Araújo, A., Ditas, F., Holanda, B. A., Sá, M. O., Tsokankunku, A., Walter, D., Wolff, S., Lavrič, J. V., Pöhlker, C., Sörgel, M., and Williams, J.: Total OH reactivity over the Amazon rainforest: variability with temperature, wind, rain, altitude, time of day, season, and an overall budget closure, Atmos. Chem. Phys., 21, 6231–6256, https://doi.org/10.5194/acp-21-6231-2021, 2021.

Pierotti, D., Wofsy, S. C., Jacob, D., and Rasmussen, R. A.: Isoprene and its oxidation products: Methacrolein and methyl vinyl ketone, J. Geophys. Res.-Atmos., 95, 1871–1881, https://doi.org/10.1029/JD095iD02p01871, 1990.

Pöhlker, C., Walter, D., Paulsen, H., Könemann, T., Rodríguez-Caballero, E., Moran-Zuloaga, D., Brito, J., Carbone, S., Degrendele, C., Després, V. R., Ditas, F., Holanda, B. A., Kaiser, J. W., Lammel, G., Lavrič, J. V., Ming, J., Pickersgill, D., Pöhlker, M. L., Praß, M., Löbs, N., Saturno, J., Sörgel, M., Wang, Q., Weber, B., Wolff, S., Artaxo, P., Pöschl, U., and Andreae, M. O.: Land cover and its transformation in the backward trajectory footprint region of the Amazon Tall Tower Observatory, Atmos. Chem. Phys., 19, 8425–8470, https://doi.org/10.5194/acp-19-8425-2019, 2019.

Pugliese, G., Ingrisch, J., Meredith, L. K., Pfannerstill, E. Y., Klüpfel, T., Meeran, K., Byron, J., Purser, G., Gil-Loaiza, J., van Haren, J., Dontsova, K., Kreuzwieser, J., Ladd, S. N., Werner, C., and Williams, J.: Effects of drought and recovery on soil volatile organic compound fluxes in an experimental rainforest, Nat. Commun., 14, 5064, https://doi.org/10.1038/s41467-023-40661-8, 2023.

Ringsdorf, A., Edtbauer, A., Holanda, B., Poehlker, C., Sá, M. O., Araújo, A., Kesselmeier, J., Lelieveld, J., and Williams, J.: Investigating carbonyl compounds above the Amazon rainforest using a proton-transfer-reaction time-of-flight mass spectrometer (PTR-ToF-MS) with NO^+ chemical ionization, Atmos. Chem. Phys., 24, 11883–11910, https://doi.org/10.5194/acp-24-11883-2024, 2024.

Rinnan, R. and Albers, C. N.: Soil Uptake of Volatile Organic Compounds: Ubiquitous and Underestimated?, J. Geophys. Res.-Biogeo., 125, e2020JG005773, https://doi.org/10.1029/2020JG005773, 2020.

Rinne, H. J. I., Guenther, A. B., Greenberg, J. P., and Harley, P. C.: Isoprene and monoterpene fluxes measured above Amazonian rainforest and their dependence on light and temperature, Atmos. Environ., 36, 2421–2426, https://doi.org/10.1016/S1352-2310(01)00523-4, 2002.

Rizzo, L. V., Artaxo, P., Karl, T., Guenther, A. B., and Greenberg, J.: Aerosol properties, in-canopy gradients, turbulent fluxes and VOC concentrations at a pristine forest site in Amazonia, Atmos. Environ., 44, 503–511, https://doi.org/10.1016/j.atmosenv.2009.11.002, 2010.

Sarkar, C., Guenther, A. B., Park, J.-H., Seco, R., Alves, E., Batalha, S., Santana, R., Kim, S., Smith, J., Tóta, J., and Vega, O.: PTR-TOF-MS eddy covariance measurements of isoprene and monoterpene fluxes from an eastern Amazonian rainforest, Atmos. Chem. Phys., 20, 7179–7191, https://doi.org/10.5194/acp-20-7179-2020, 2020.

Schmidt, R., Cordovez, V., de Boer, W., Raaijmakers, J., and Garbeva, P.: Volatile affairs in microbial interactions, ISME J., 9, 2329–2335, https://doi.org/10.1038/ismej.2015.42, 2015.

Schüttler, J. M., Pugliese, G., Byron, J., and Williams, J.: Soil fluxes and volume mixing ratios (VMR) of volatile organic compounds (VOCs) measured at the ATTO Site in 2023 and 2024, Max Planck Institute for Biogeochemistry [data set], https://doi.org/10.17871/ATTO.612.7.2472, 2025.

Schulz-Bohm, K., Geisen, S., Wubs, E. R. J., Song, C., de Boer, W., and Garbeva, P.: The prey's scent – Volatile organic compound mediated interactions between soil bacteria and their protist predators, ISME J., 11, 817–820, https://doi.org/10.1038/ismej.2016.144, 2017.

Song, W., Staudt, M., Bourgeois, I., and Williams, J.: Laboratory and field measurements of enantiomeric monoterpene emissions as a function of chemotype, light and temperature, Biogeosciences, 11, 1435–1447, https://doi.org/10.5194/bg-11-1435-2014, 2014.

Staudt, M., Bourgeois, I., Al Halabi, R., Song, W., and Williams, J.: New insights into the parametrization of temperature and light responses of mono – and sesquiterpene emissions from Aleppo pine and rosemary, Atmos. Environ., 152, 212–221, https://doi.org/10.1016/j.atmosenv.2016.12.033, 2017.

Staudt, M., Byron, J., Piquemal, K., and Williams, J.: Compartment specific chiral pinene emissions identified in a Maritime pine forest, Sci. Total Environ., 654, 1158–1166, https://doi.org/10.1016/j.scitotenv.2018.11.146, 2019.

Tang, J., Schurgers, G., and Rinnan, R.: Process Understanding of Soil BVOC Fluxes in Natural Ecosystems: A Review, Rev. Geophys., 57, 966–986, https://doi.org/10.1029/2018RG000634, 2019.

Tani, A., Tobe, S., and Shimizu, S.: Uptake of Methacrolein and Methyl Vinyl Ketone by Tree Saplings and Implications for Forest Atmosphere, Environ. Sci. Technol., 44, 7096–7101, https://doi.org/10.1021/es1017569, 2010.

Tripathi, N., Krumm, B. E., Edtbauer, A., Ringsdorf, A., Wang, N., Kohl, M., Vella, R., Machado, L. A. T., Pozzer, A., Lelieveld, J., and Williams, J.: Impacts of convection, chemistry, and forest clearing on biogenic volatile organic compounds over the Amazon, Nat. Commun., 16, 4692, https://doi.org/10.1038/s41467-025-59953-2, 2025.

Tsuruta, J., Okumura, M., Makita, N., Kosugi, Y., Miyama, T., Kume, T., and Tohno, S.: A comparison of the biogenic volatile organic compound emissions from the fine roots of 15 tree species in Japan and Taiwan, J. For. Res.-Jpn., 23, 242–251, https://doi.org/10.1080/13416979.2018.1483129, 2018.

Ueda, H., Kikuta, Y., and Matsuda, K.: Plant communication: Mediated by individual or blended VOCs?, Plant Signaling & Behavior, 7, 222–226, https://doi.org/10.4161/psb.18765, 2012.

Vance, E. D., Brookes, P. C., and Jenkinson, D. S.: An extraction method for measuring soil microbial biomass C, Soil Biol. Biochem., 19, 703–707, https://doi.org/10.1016/0038-0717(87)90052-6, 1987.

Vella, R., Pozzer, A., Forrest, M., Lelieveld, J., Hickler, T., and Tost, H.: Changes in biogenic volatile organic compound emissions in response to the El Niño–Southern Oscillation, Biogeosciences, 20, 4391–4412, https://doi.org/10.5194/bg-20-4391-2023, 2023.

Viros, J., Santonja, M., Temime-Roussel, B., Wortham, H., Fernandez, C., and Ormeño, E.: Volatilome of Aleppo Pine litter over decomposition process, Ecol. Evol., 11, 6862–6880, https://doi.org/10.1002/ece3.7533, 2021.

Weikl, F., Ghirardo, A., Schnitzler, J.-P., and Pritsch, K.: Sesquiterpene emissions from Alternaria alternata and Fusarium oxysporum: Effects of age, nutrient availability and co-cultivation, Sci. Rep., 6, 22152, https://doi.org/10.1038/srep22152, 2016.

Werner, C., Meredith, L. K., Ladd, S. N., and the B2WALD: Ecosystem BVOC fluxes during drought and recovery trace ecohydrological responses of the vegetation and soil microbial interactions - insights from an ecosystem-scale isotope labelling experiment, EGU General Assembly 2022, Vienna, Austria, 23–27 May 2022, EGU22-11637, https://doi.org/10.5194/egusphere-egu22-11637, 2022.

White, C. S.: The role of monoterpenes in soil nitrogen cycling processes in ponderosa pine, Biogeochemistry, 12, 43–68, https://doi.org/10.1007/BF00002625, 1991.

White, D. C.: Chemical Ecology: Possible Linkage between Macro- and Microbial Ecology, Oikos, 74, 177–184, https://doi.org/10.2307/3545646, 1995.

Williams, J.: Organic Trace Gases in the Atmosphere: An Overview, Environ. Chem., 1, 125–136, https://doi.org/10.1071/EN04057, 2004.

Williams, J., Yassaa, N., Bartenbach, S., and Lelieveld, J.: Mirror image hydrocarbons from Tropical and Boreal forests, Atmos. Chem. Phys., 7, 973–980, https://doi.org/10.5194/acp-7-973-2007, 2007.

Yáñez-Serrano, A. M., Nölscher, A. C., Williams, J., Wolff, S., Alves, E., Martins, G. A., Bourtsoukidis, E., Brito, J., Jardine, K., Artaxo, P., and Kesselmeier, J.: Diel and seasonal changes of biogenic volatile organic compounds within and above an Amazonian rainforest, Atmos. Chem. Phys., 15, 3359–3378, https://doi.org/10.5194/acp-15-3359-2015, 2015.

Yáñez-Serrano, A. M., Nölscher, A. C., Bourtsoukidis, E., Gomes Alves, E., Ganzeveld, L., Bonn, B., Wolff, S., Sa, M., Yamasoe, M., Williams, J., Andreae, M. O., and Kesselmeier, J.: Monoterpene chemical speciation in a tropical rainforest:variation with season, height, and time of dayat the Amazon Tall Tower Observatory (ATTO), Atmos. Chem. Phys., 18, 3403–3418, https://doi.org/10.5194/acp-18-3403-2018, 2018.

Yáñez-Serrano, A. M., Mahlau, L., Fasbender, L., Byron, J., Williams, J., Kreuzwieser, J., and Werner, C.: Heat stress increases the use of cytosolic pyruvate for isoprene biosynthesis, J. Exp. Bot., 70, 5827–5838, https://doi.org/10.1093/jxb/erz353, 2019.

Yáñez-Serrano, A. M., Bourtsoukidis, E., Alves, E. G., Bauwens, M., Stavrakou, T., Llusià, J., Filella, I., Guenther, A., Williams, J., Artaxo, P., Sindelarova, K., Doubalova, J., Kesselmeier, J., and Peñuelas, J.: Amazonian biogenic volatile organic compounds under global change, Global Change Biol., 26, 4722–4751, https://doi.org/10.1111/gcb.15185, 2020.

Yang, K., Llusià, J., Preece, C., Ogaya, R., Márquez Tur, L., Mu, Z., You, C., Xu, Z., Tan, Y., and Peñuelas, J.: Impacts of seasonality, drought, nitrogen fertilization, and litter on soil fluxes of biogenic volatile organic compounds in a Mediterranean forest, Sci. Total Environ., 906, 167354, https://doi.org/10.1016/j.scitotenv.2023.167354, 2024.

Yassaa, N. and Williams, J.: Enantiomeric monoterpene emissions from natural and damaged Scots pine in a boreal coniferous forest measured using solid-phase microextraction and gas chromatography/mass spectrometry, J. Chromatogr. A., 1141, 138–144, https://doi.org/10.1016/j.chroma.2006.12.006, 2007.

Yee, L. D., Isaacman-VanWertz, G., Wernis, R. A., Meng, M., Rivera, V., Kreisberg, N. M., Hering, S. V., Bering, M. S., Glasius, M., Upshur, M. A., Gray Bé, A., Thomson, R. J., Geiger, F. M., Offenberg, J. H., Lewandowski, M., Kourtchev, I., Kalberer, M., de Sá, S., Martin, S. T., Alexander, M. L., Palm, B. B., Hu, W., Campuzano-Jost, P., Day, D. A., Jimenez, J. L., Liu, Y., McKinney, K. A., Artaxo, P., Viegas, J., Manzi, A., Oliveira, M. B., de Souza, R., Machado, L. A. T., Longo, K., and Goldstein, A. H.: Observations of sesquiterpenes and their oxidation products in central Amazonia during the wet and dry seasons, Atmos. Chem. Phys., 18, 10433–10457, https://doi.org/10.5194/acp-18-10433-2018, 2018.

Zannoni, N., Leppla, D., Lembo Silveira de Assis, P. I., Hoffmann, T., Sá, M., Araújo, A., and Williams, J.: Surprising chiral composition changes over the Amazon rainforest with height, time and season, Commun. Earth Environ., 1, 1–11, https://doi.org/10.1038/s43247-020-0007-9, 2020.